



Cite this: *Chem. Commun.*, 2019, 55, 9251

Received 20th May 2019,  
Accepted 2nd July 2019

DOI: 10.1039/c9cc03910d

rsc.li/chemcomm

# Which future for stereogenic phosphorus? Lessons from P\* pincer complexes of iron(II)

Raffael Huber,  Alessandro Passera  and Antonio Mezzetti  \*

PNP pincer ligands stabilise diamagnetic base metal catalysts, and much effort has been invested in the development of chiral analogues for asymmetric catalysis. Starting from the conformational issues that affect P-stereogenic diphosphines, we extend the analysis to our recently prepared P-stereogenic PNP pincer ligands, which we used in the iron(II)-catalysed hydrogenation of ketones. Backbone rigidity and size (and shape) of the substituents at phosphorus are pivotal in both bi- and tridentate P-stereogenic ligands, and their interplay is discussed, as well as the contribution (and shortcomings) of DFT calculations to the understanding of the conformational flexibility and enantiodiscrimination.

## Iron(II) and stereogenic phosphorus: the context

### Scope and goal

Pincer ligands form robust complexes with base metals and have hence played a pivotal role in the development of base metal catalysts. In these studies, a handful of C-stereogenic pincer ligands have been developed prior to our study. Stereogenic phosphorus (P\*) has met large success in combination with bidentate ligands,<sup>1</sup> but had not been used with tridentate ligands for base metal catalysts. Our group has prepared P-stereogenic PNP pincer ligands and used them in the iron-catalysed asymmetric hydrogenation of ketones.

The goal of this article is to put the conformational issues encountered during our study in a broader context that encompasses P-stereogenic diphosphines and (the few) PNP/PCP pincer catalysts of other metals, both precious and non-noble.

### The new Frontier: chiral ligands for base metal catalysts

**Iron as a pioneer.** Much effort has been spent in developing homogeneous catalysts based on cheap, low toxic base metals.<sup>2</sup> In this endeavour, iron has played a pioneering role.<sup>3</sup> From the original interest in C–C bond formation, in which the nature of the iron catalyst is elusive,<sup>4</sup> the focus has progressively shifted to reactions that require a well-defined catalytically active species, such as the enantioselective hydrogenation of polar double bonds. This key technology gives access to chiral building blocks for chemical synthesis,<sup>5</sup> and the industry is actively

Department of Chemistry and Applied Biosciences, ETH Zürich, Wolfgang-Pauli-Str. 10, CH-8093 Zürich, Switzerland. E-mail: mezzetti@inorg.chem.ethz.ch



Raffael Huber

*Raffael Huber, born 1992 in Altdorf (Switzerland) studied chemistry at the ETH Zürich. After his Master degree in 2014 with Prof. Antonio Mezzetti on NPPN iron(II) complexes, he obtained his PhD degree in the same group in 2018 with a thesis on P-stereogenic pincer ligands in iron-catalysed reactions.*



Alessandro Passera

*Alessandro Passera was born in Magenta (Italy) in 1992. After a MSc thesis co-supervised by Prof. Anna Iuliano (University of Pisa, Italy) and Prof. Vincenzo Passarelli (University of Zaragoza, Spain), Alessandro Passera concluded his Chemistry study with the Diploma of Sciences at the Scuola Normale Superiore in Pisa. He is now PhD student at ETH Zürich under the supervision of Prof. Antonio Mezzetti. His current research is focused on Mn(I) and Fe(II) catalysts for the asymmetric hydrogenation of ketones.*



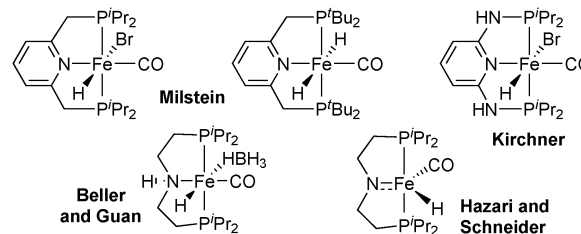
seeking for catalytic processes with affordable costs to replace stoichiometric processes or precious metal catalysts.<sup>6</sup>

The first iron(II) catalysts for the asymmetric hydrogenation of polar double bonds have been designed by analogy with their ruthenium(II) analogues.<sup>7</sup> Thus, the first asymmetric iron(II) catalyst for the hydrogenation of ketones, reported by Morris in 2008,<sup>8</sup> was based on the tetradentate, open-chain PNNP ligand already used with ruthenium and exploited in hydrogen transfer from 2-propanol.<sup>7b</sup> It should be noted, however, that the analogy between iron(II) and ruthenium(II) is deceiving, as iron(II) complexes are considerably less stable than their heavier counterparts. However, the combination of good  $\sigma$  donors, such as phosphines, with strong  $\pi$ -accepting ancillary ligands, *e.g.* CO, stabilises the low spin  $d^6$  configuration in which all M–L  $\sigma^*$  antibonding orbitals are empty. Hence, ligand lability can be greatly reduced, and robust complexes are obtained.

For instance, Morris' second-generation PNNP catalyst ligand is stable, but yet active and achieves turnover frequencies of up to  $200\text{ s}^{-1}$ .<sup>9</sup> With the same goal, our group has developed macrocyclic  $N_2P_2$  ligands that, combined with isonitriles as ancillary ligands, form robust, highly enantioselective catalysts for the transfer hydrogenation of a broad scope of ketones, including a hydride complex that catalyses the base-free reduction of benzils.<sup>10</sup>

As already observed for ruthenium(II),<sup>11</sup> the complexes of tetradentate  $N_2P_2$  ligands perform well in transfer hydrogenation, but are poor catalysts for the hydrogenation with  $H_2$ ,<sup>12</sup> which is preferable for industrial application due to its irreversibility and atom economy.

**Achiral and C-stereogenic pincer ligands.** Again, to develop iron(II) catalysts for the pressure hydrogenation of ketones, the inspiration came from ruthenium, and in particular from its pincer PNP complexes, which are excellent catalysts for various (de)hydrogenation reactions.<sup>13</sup> The field was pioneered by Milstein<sup>14</sup> with 2,6-dimethylenepyridine as a non-innocent<sup>15</sup> PNP framework. In 2011, he reported an iron/PNP pincer



Scheme 1 Achiral Fe/PNP catalysts for direct hydrogenation.

bromocarbonylhydride that catalyses the hydrogenation of ketones at remarkably low loading (0.05 mol%), room temperature, and low  $H_2$  pressure (4 atm).<sup>16</sup> The same catalyst also hydrogenates aldehydes<sup>17</sup> and amides,<sup>18</sup> and an analogous dihydride complex (Scheme 1) reduces trifluoroacetic esters to the corresponding alcohols.<sup>19</sup> Similarly, Kirchner showed that iron(II) complexes of the 2,6-diaminopyridine analogue catalyse the hydrogenation of ketones and aldehydes.<sup>20</sup>

As an alternative to the pyridine backbone, Beller<sup>21</sup> and Guan<sup>22</sup> have used a *N,N*-diethylenamine bridge for PN(H)P pincer ligands whose iron borohydridecarbonylhydride complex catalyses the hydrogenation of esters (Scheme 1). The secondary amine in the backbone directs and activates the carbonyl group towards hydride attack in the bifunctional mechanism.<sup>23</sup> Jones extended the use of this catalyst to the acceptorless dehydrogenation and hydrogenation of *N*-heterocycles,<sup>24</sup> and Hazari and Schneider reported a five-coordinate iron carbonylhydride that catalyses the acceptorless dehydrogenation of alcohols as well as ketone hydrogenation.<sup>25</sup>

All PNP pincer complexes described so far were achiral. In 2014, Morris reported the first iron(II) catalyst for the asymmetric pressure hydrogenation of ketones, a PNP bromocarbonyl complex with an enantiopure 1-methyl-2-phenylethylene chelate that hydrogenates acetophenone with 80% ee (Scheme 2).<sup>26</sup>

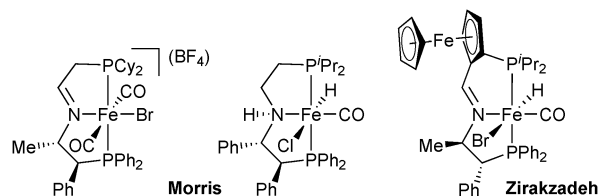
A second-generation chlorocarbonylhydride complex reduces acetophenone with 95% ee.<sup>27</sup> This catalyst also reduces the heterocyclic 2-acetylfuran with full conversion and 95% ee. The more acidic 3,5-bis(trifluoromethyl)acetophenone and also the bulkier cyclohexyl phenyl ketone are not tolerated, however, and lead to low conversion (8% and 38%, respectively). Zirakzadeh introduced ferrocenyl as an additional stereogenic element, and the corresponding bromocarbonylhydride complex is an active catalyst for the hydrogenation of arylalkyl ketones (81% ee for acetophenone, Scheme 2).<sup>28</sup>

The catalysts shown in Scheme 2 all contain C-stereogenic ligands and have achieved notable enantioselectivity in selected



Antonio Mezzetti

Antonio Mezzetti was born in Trieste (Italy) in 1958, where he completed his studies in chemistry. In 1986, he joined the Chemistry Department of the University of Udine as Research Associate. After sabbatical stays at the ETH Zurich with Prof. Giambattista Consiglio and the late Prof. Luigi M. Venanzi, he joined the Laboratory of Inorganic Chemistry of the ETH Zürich in 1995, where he is now Titular Professor. His research interests are at the interface between coordination chemistry and homogeneous catalysis.



Scheme 2 Iron catalysts for enantioselective direct hydrogenation.



instances, but their substrate scope is still narrow. In the quest for improvement, we have developed iron(II) catalysts with P-stereogenic pincer ligands and either pyridine (PNP) or *N,N*-diethyleneamine (PN(H)P) backbones. For this study, we chose dialkylphosphino units by analogy with the highly successful achiral iron(II) catalysts with pincer ligands.

An inherent difficulty of pyridine-based pincers (such as in Scheme 1 top) is that the benzylic position of the backbone is most likely to undergo deprotonation during catalysis, and a stereocentre in this position would be quickly epimerised. Hence, P-based stereocentres seemed particularly suitable. The lessons we learnt from these new PNP pincer ligands reminded us of the conformational issues that are also found in P-stereogenic diphosphines, which are recapitulated in the next section, starting with a detour to ligands with carbon based stereocentres.

## P\* diphosphines: conformational issues

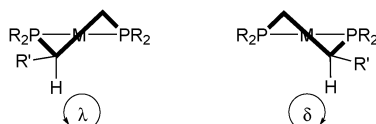
### Introduction

Restricted conformational ligand flexibility has long been considered as the key factor to achieve high enantioselectivity in catalysis, and many rigid structures from the chiral pool have been used as backbones.<sup>29</sup> The introduction of a chelate ring between two phosphine donors is the first step toward rigidifying the system. However, chelate rings are intrinsically flexible. The classical approach to lock the conformation of the chelate ring is to introduce substituents into the P–P chelate to give C-stereogenic diphosphines. To understand the fundamental difference between P- and C-stereogenic ligands, it is necessary to examine the factors that steer the conformation of C-stereogenic ligands.

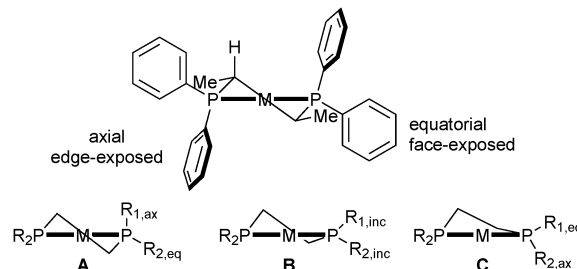
### Five-membered chelate rings

For diphosphine ligands that contain  $\text{PPh}_2$  donors, it has been recognized early that enantioselection derives from the chiral conformation of the phenyl rings, which, in the case of C-stereogenic diphosphines, is dictated by the stereocentres in the chelate.<sup>30</sup> The absolute configuration of five-membered rings ( $\lambda$  or  $\delta$ ) is controlled by the preference of the (larger) substituents for equatorial positions (Scheme 3, the  $\text{R}'$  substituent is given the third priority in the CIP rules).<sup>31</sup> Therefore, the backbones of diphosphines with *R* stereocentres typically lead to a  $\lambda$  conformation, and *S* configured ones give  $\delta$  conformations.

In turn, the conformation of the chelate determines the orientation of the phenyl rings, which transmit the chiral



**Scheme 3** Illustration of  $\lambda$  (left) and  $\delta$  (right) conformations in five-membered chelate rings.



**Scheme 4** Chelate and phenyl conformation in Chiraphos.

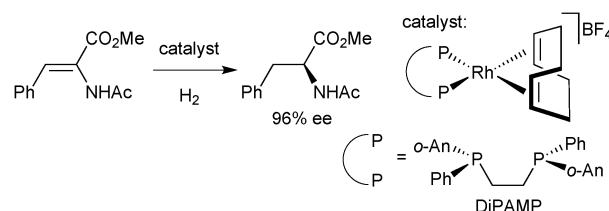
information to the metal-bound substrate, leading to enantioselection. In Prophos and Chiraphos, an analysis of several crystal structures indicates that the axial phenyl is preferentially edge exposed and hence interacts with the substrate more strongly than the equatorial phenyl, which tends to be face exposed (Scheme 4 top).<sup>32</sup> However, there is a certain degree of conformational flexibility, and three types of conformations have been observed for diphosphines that form five-membered chelates such as Chiraphos (Scheme 4).<sup>32</sup>

In the half-chair conformation (A), the substituents on phosphorus are clearly distinguishable as equatorial and axial and are arranged in an approximately  $C_2$ -symmetric fashion. In structures close to an envelope conformation (B), which have a small  $\text{P–M–P}_{\text{ring}}$  torsion angle  $\alpha$ , the substituents on the in-plane P atom are best described as inclinal ( $R_{\text{inc}}$  in Scheme 4). In further distorted envelope conformations (C), the sign of the torsion angle  $\alpha$  is inverted, and the axial and equatorial positions of the phosphorus substituents are switched with respect to A. A correlation between axial/equatorial and edge/face-exposed is possible only in half-chair structure A or in envelope structure C with a large torsion angle  $\alpha$  ( $\text{P–M–P}_{\text{ring}}$ ).<sup>32</sup>

### P-Stereogenic diphosphines with small chelates

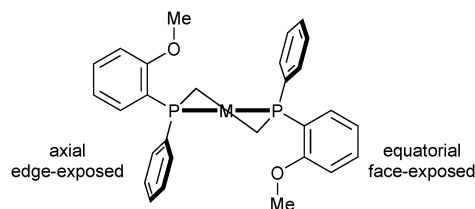
The interest in P-stereogenic ligands was triggered by Knowles' hydrogenation of  $\alpha$ -acylaminocinnamates catalysed by Rh/DiPAMP (Scheme 5).<sup>33</sup>

The mechanistic investigations of enamide hydrogenation have revealed intricacies that are still a matter of debate,<sup>34,35</sup> but have also showed that the conformation of the chelate ring is significantly more flexible in DiPAMP than in Chiraphos.<sup>36</sup> Also, one should keep in mind that the roles of the backbone and of the phosphorus substituents are reversed in P-stereogenic diphosphines as compared to C-stereogenic ligands with  $\text{PPh}_2$  donors such as Chiraphos. Indeed, in P-stereogenic ligands, the



**Scheme 5** Asymmetric hydrogenation of methyl-(*Z*)- $\alpha$ -acetamidocinnamate with Rh/DiPAMP.



Scheme 6 Chelate and phenyl/*o*-anisyl conformation in DiPAMP.

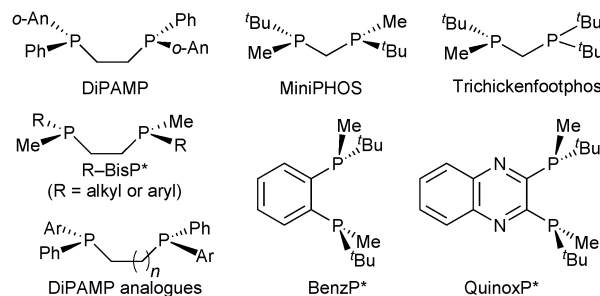
substituents at phosphorus play a dual role as they generate the chiral environment for the approach of the substrate and lock the conformation of the chelate ring according to their size. This can lead to some confusion. Thus, in DiPAMP, the *o*-anisyl group acts as the “large” substituent in the chelate and hence occupies its equatorial position, but is “small” with respect to the substrate, as it is face exposed (Scheme 6). In contrast, the smaller phenyl group is axial, but edge exposed toward the substrate, and thus acts as the bulky group toward the metal-bound substrate.<sup>35</sup> With the so-called quadrant rule, Knowles has attempted to correlate empirically the spatial arrangement of the substituents on P in the catalyst precursor (usually a diolefin complex) with the absolute configuration of the protected amino acid obtained from enamide hydrogenation.<sup>37</sup>

However, the overall crowding in the complex affects the subtle interplay between the conformation of the chelate and the orientation of the substituents on phosphorus. Thus, the same P-stereogenic phosphine assumes opposite conformations in its norbornadiene and 1,5-cyclooctadiene complexes, but gives the same sense of induction in the hydrogenation of dehydro amino acids.<sup>38</sup>

Moreover, polysubstituted aryl substituents on phosphorus favour envelope conformations such as B and C in Scheme 4, which is beneficial for enantioselectivity, but hinders the development of simple rules-of-thumb.<sup>39</sup> The conformational issue is acute also when the size of the P-substituents is similar, as in the case of (*S,S*)-<sup>t</sup>Bu(Ph)PCH<sub>2</sub>CH<sub>2</sub>P(<sup>t</sup>Bu)Ph,<sup>40</sup> whose complexes show a flattened conformation of the chelate ring with no clear axial/equatorial distinction of the *tert*-butyl and phenyl groups. Accordingly, the <sup>t</sup>Bu-substituted ligand gives the lowest enantioselectivity in the series R(Ph)PCH<sub>2</sub>CH<sub>2</sub>P(R)Ph (R = <sup>t</sup>Bu, *o*-anisyl, 1-naphthyl).<sup>40</sup>

Therefore, the substituents on stereogenic P atoms should be significantly different in size. The P(<sup>t</sup>Bu)Me unit meets this requirement, as the *tert*-butyl group has cylindrical symmetry with respect to P–<sup>t</sup>Bu rotation and is always larger as compared to the methyl group. Imamoto's ethane-1,2-diyl-bridged, P-stereogenic diphosphines BisP\* with alkylmethyl- or arylmethylphosphine donors (Scheme 7) are a privileged class of ligands and provide excellent enantioselectivity with a wide variety of catalytic reactions.<sup>41</sup>

The X-ray structures and DFT calculations of <sup>t</sup>Bu–BisP\* complexes exclusively show conformations with the bulky group in the equatorial position,<sup>35</sup> but the enantioselectivity of BisP\* rhodium catalysts strongly depends on the structure of the substrate.<sup>42</sup> Therefore, more rigid backbones were



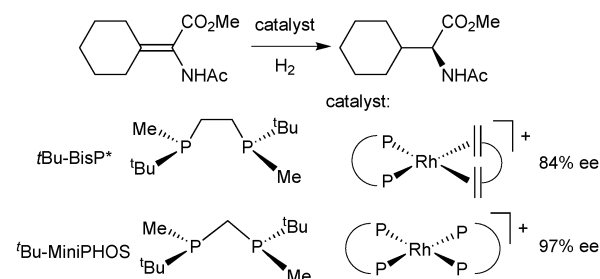
Scheme 7 Some frequently used P-stereogenic ligands.

introduced to improve the control of the conformation of the chelate during catalysis. In a first approach, Imamoto used a shorter chelate backbone for ligands of the general formula Me(R)P–CH<sub>2</sub>–P(Me)R (Scheme 8).<sup>43</sup> The four-membered chelate ring formed upon complexation is conformationally rigid and almost perfectly planar.<sup>42</sup> MiniPHOS rhodium catalysts outperform BisP\* ligands in the hydrogenation of β,β-disubstituted dehydro amino acids (Scheme 8).<sup>42</sup>

However, MiniPHOS gives lower enantioselectivity than BisP\* in the rhodium-catalysed hydrogenation of unsubstituted enamides,<sup>44</sup> possibly because its smaller bite angle (*ca.* 72°) reduces the overall steric bulk. In the *C*<sub>1</sub>-symmetric modified MiniPHOS-type ligand <sup>t</sup>Bu<sub>2</sub>PCH<sub>2</sub>P(CH<sub>3</sub>)<sup>t</sup>Bu (Trichickenfootphos, Scheme 7), the large achiral P<sup>t</sup>Bu<sub>2</sub> donor apparently compensates for the effect of the small chelate and gives excellent enantioselectivity with dehydro amino acid derivatives.<sup>45</sup> The NH-bridged MaxPHOS (RR'P\*–NH–P\*RR') is also a MiniPHOS derivative.<sup>46</sup>

An alternative strategy to rigidify P-stereogenic diphosphines with a five-membered chelate, such as BisP\*, is the use of a 1,2-phenylene linker instead of ethane-1,2-diyl. With ligands bearing pseudo-chirality<sup>47</sup> on phosphorus such as DuPHOS and BPE, this approach has improved the enantioselectivity of the Rh-catalysed asymmetric hydrogenation of α-acetamidoacrylates (Scheme 9).<sup>48</sup>

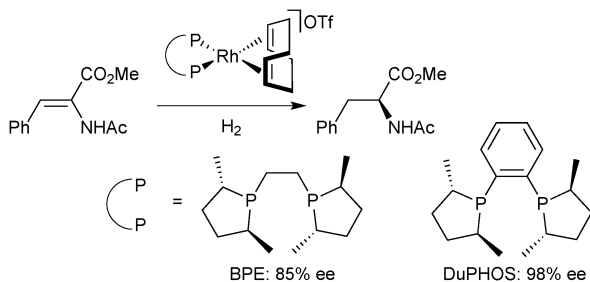
On this track, Imamoto prepared P-stereogenic ligands with a 1,2-phenylene backbone such as BenzP\*<sup>49</sup> and QuinoxP (Scheme 7).<sup>50</sup> In the hydrogenation of (*Z*)-methyl 3-acetamidobut-2-enoate, the enantioselectivity dramatically increased from 19.7% ee with <sup>t</sup>Bu–BisP\*<sup>41c</sup> to 97.6% ee with BenzP\* (Scheme 10).<sup>49b</sup> BenzP\* and QuinoxP\* have found broad application in asymmetric catalysis, such as Rh-catalysed asymmetric hydrogenation<sup>51</sup> and



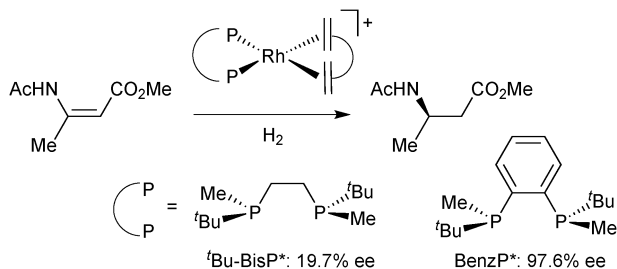
Scheme 8 Asymmetric hydrogenation of methyl 2-acetamido-2-cyclohexylideneacetate.







**Scheme 9** Effect of the linker rigidity on the asymmetric hydrogenation with non-P-stereogenic diphosphines.



**Scheme 10** Asymmetric hydrogenation of methyl-(Z)-3-acetamidobut-2-enoate.

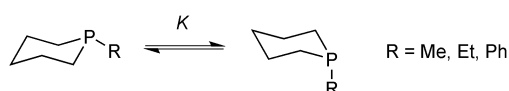
hydroacylation,<sup>52</sup> in Cu-catalysed arylation<sup>53</sup> and borylation<sup>54</sup> reactions, Pd-catalysed allylic alkylations,<sup>55</sup> and Fe-catalysed cross coupling.<sup>56</sup>

### Diphosphines with larger chelates

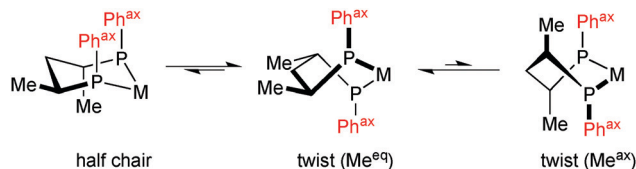
In the context of six-membered phosphacycles, it should be mentioned that caution is required when discussing the conformations of chelate rings formed by multidentate P-stereogenic phosphine ligands, as they lack the strong bias towards the equatorial conformer that is typical of cyclohexanes. This is illustrated by the conformational equilibrium of the phosphinanes (Scheme 11).<sup>57</sup>

In these molecules, the entropic preference for the axial conformation is larger than in cyclohexanes, and the corresponding  $\Delta H$  and  $\Delta S$  values are similar. Hence, the equilibrium constant  $K$  for the equatorial/axial equilibrium depends more strongly on temperature. Also, the axial isomer shows weaker 1,3-diaxial interactions because the P–C bonds are longer than C–C. Hence, for 1-methyl, 1-ethyl, and 1-phenyl phosphinanes, the axial conformer is in excess at room temperature.

Back to diphosphines, we have seen above that the most successful P-stereogenic ligands form small chelate rings upon coordination (five- or four-membered, Scheme 8). Six-membered chelate rings have been used with some success in combination with P-stereogenic diarylphosphine donors,<sup>58</sup>



**Scheme 11** Conformational equilibrium in phosphinanes.



**Scheme 12** Conformations of (2S,4S)-[RhL<sub>2</sub>(bdpp)]<sup>+</sup> (only one of the two equivalent half chair conformations is shown).

whereas dialkylphosphine donors have been found to give low enantioselectivity.<sup>59</sup> This is unsurprising, as six-membered chelate rings are intrinsically more flexible than smaller ones. The typical example is 2,4-bis(diphenylphosphino)pentane (bdpp), which forms, besides the most stable twist conformation with all-equatorial methyl groups, an energetically accessible achiral half-chair in which the axial substituents on phosphorus assume an achiral conformation (Scheme 12).<sup>60</sup>

To rigidify P-stereogenic diphosphines with six-membered chelate rings, *gem*-disubstitution on the central atom of the backbone was attempted with success with diarylphosphine donors, such as in Me<sub>2</sub>Si(CH<sub>2</sub>P(1-Np)Ph)<sub>2</sub>,<sup>61</sup> but failed with dialkylphosphines.<sup>59</sup> Also, as seen above for five-membered rings, the use of aromatic backbones is beneficial for enantioselectivity. Thus, P-stereogenic diphosphines featuring larger chelates take advantage of rigid xanthene structures.<sup>62</sup> With the aim of increasing the bite angle of the P-stereogenic diphosphine, ferrocene-1,1'-diyl also has been used as the backbone, and the resulting ligands give high enantioselectivity in the rhodium-catalysed hydrogenation of acetamido cinnamates and other functionalized alkenes,<sup>63</sup> but the rotation of the cyclopentadienyl rings of the ferrocene bridge allows for several conformations of the ligand, as observed by <sup>31</sup>P NMR spectroscopy in solution.<sup>63b</sup> Interestingly, a recent application of a P(<sup>t</sup>Bu)Me/oxazoline ligand in the iridium-catalysed hydrogenation of *N*-alkyl imines suggests that P-stereogenic phosphines also give stiff conformations in the presence of an external rigidifying element, in this case, a cyclometalated benzimine.<sup>64</sup>

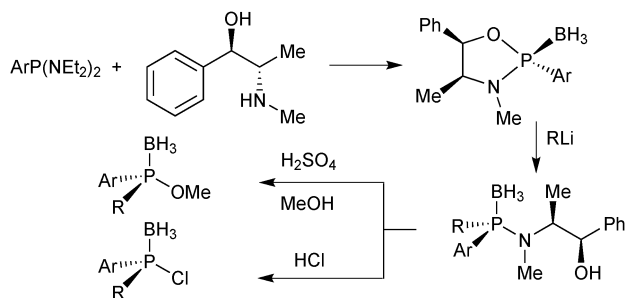
Overall, the above discussion shows that the conformational issues of P-stereogenic diphosphines play a pivotal role in enantiodiscrimination. Before extending it to tridentate ligands, the synthetic protocols for P-stereogenic building blocks are recapitulated in the next section.

## P-Stereogenic synthons

### General remarks

The lack of adequate synthetic methods has long been the bottleneck for the application of P-stereogenic ligands in homogeneous catalysis. Therefore, the three established pathways presented in the next section have made a major contribution to alleviate this issue, and the timeline of their development (late 1990s and 2000s) directly precedes the resurgence of catalysts with P-stereogenic ligands. These methods are based on Jugé and Stephan's 1,3,2-oxazaphospholidine boranes derived from ephedrine,<sup>65</sup> Evans<sup>66</sup> and Imamoto's<sup>67</sup>





**Scheme 13** Jugé's enantiomerically pure aminophosphine and phosphinite boranes.

enantioselective deprotonation of phosphine boranes with sparteine, and Mislow and Han's menthyl phosphinates.<sup>68</sup> For an exhaustive review of all known synthetic methods, the reader is referred to dedicated surveys.<sup>1</sup>

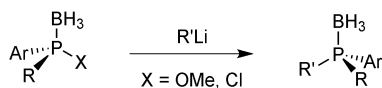
### 1,3,2-Oxazaphospholidine boranes

In Jugé's method, enantiomerically pure phosphines are prepared from an aryl diaminephosphine and ephedrine *via* a 1,3,2-oxazaphospholidine borane.<sup>65</sup> Ring-opening of oxazaphospholidine boranes with a wide scope of organolithium reagents<sup>65c</sup> gives the corresponding aminophosphine boranes (Scheme 13).

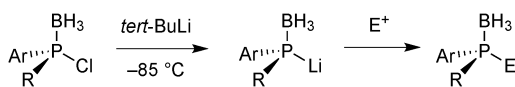
Also bulky alkyl lithium reagents can be used,<sup>39</sup> but supermesityllithium (2,4,6-tri-*tert*-butylphenyl lithium) or 2-adamantyl-lithium fails to give the desired product.<sup>69</sup> Organomagnesium compounds react sluggishly and require heating, which decreases the enantiospecificity.<sup>65b</sup> Usually, the aminophosphine boranes are obtained as single diastereoisomers after a simple recrystallization step. The aminophosphine is then methanolised under acidic conditions into a methyl phosphinite borane.<sup>65</sup> Alternatively, it can be treated with anhydrous HCl in an aprotic solvent such as toluene to give the more reactive chlorophosphine borane.<sup>70</sup> Both compound classes react as electrophiles, and after an  $S_N2@P$  reaction with an organolithium reagent, tertiary phosphine boranes are obtained (Scheme 14). Alkyl- as well as aryllithium reagents react with high enantiospecificity.<sup>65</sup>

One advantage of the electrophilic chlorophosphine boranes is that they undergo umpolung to nucleophilic secondary lithium phosphide boranes feasible by transmetalation with  $t^BuLi$  at  $-85^\circ C$  (Scheme 15).<sup>65c</sup>

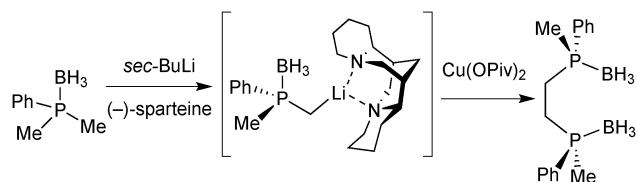
Deboronation of the final product is achieved either by reaction with an excess of amine<sup>71</sup> or by treatment with strong



**Scheme 14** Nucleophilic substitution on methyl phosphinite boranes and chlorophosphine boranes.



**Scheme 15** Umpolung of the chlorophosphine borane with  $t^BuLi$  and quenching with an electrophile.



**Scheme 16** Evans' enantioselective deprotonation with (–)-sparteine.

acids such as  $HBF_4$  etherate.<sup>72</sup> The latter method is mandatory for trialkylphosphines due to their electron-rich nature. The Jugé–Stephan method is generally applicable when at least one of the substituents in the target (tertiary) phosphine is phenyl. A drawback of the method is the use of ephedrine, which is nowadays a restricted chemical due to its use in illicit drug manufacturing.

### Enantioselective deprotonation with sparteine

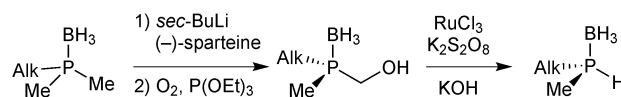
Sparteine-mediated enantioselective deprotonation has been developed by Evans and Imamoto. In 1995, Evans demonstrated that the reaction of an aryl dimethylphosphine borane with  $^sBuLi/(-)$ -sparteine leads to the enantioselective deprotonation of a methyl group, which was then exploited to prepare diphosphine ligands (Scheme 16).<sup>66</sup>

Imamoto exploited Evans' enantioselective deprotonation to prepare enantiomerically pure secondary phosphine boranes.<sup>67</sup> To this goal, the intermediate organolithium derivative was oxidised with  $O_2$  to the hydroxymethylphosphine borane with retention of configuration. Ruthenium-catalysed oxidation to the carboxylic acid and spontaneous decarboxylation under basic reaction conditions give secondary phosphine boranes with formal inversion (Scheme 17).

The secondary phosphine boranes are stable towards air and moisture, and are valuable precursors for the synthesis of a broad variety of ligands as described below.<sup>73</sup> A drawback is the stoichiometric amount of sparteine, whose (–)-enantiomer has experienced a global shortage since the early 2010s.<sup>74</sup> Nowadays, both enantiomers of the alkaloid are commercially available, at prices typical for fine chemicals.

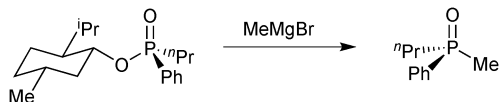
### Menthyl phosphinates

Early examples of optically active tertiary phosphines relied on resolution of the corresponding racemic oxides or quaternary phosphonium salts and subsequent reduction,<sup>75</sup> which restricts the scope of available enantiomerically pure phosphines. In 1967, Mislow tackled the problem by using menthol as a chiral auxiliary: the diastereoisomers of its phosphinate esters are easily resolved.<sup>76</sup> Substitution of the menthyl group with alkyl or aryl Grignards then gives the tertiary phosphine oxides with high stereospecificity (Scheme 18). This method enabled Knowles to prepare the DiPAMP



**Scheme 17** Imamoto's preparation of secondary phosphine boranes.





**Scheme 18** Mislow's synthesis of enantiomerically pure methylphenyl-*n*-propylphosphine oxide.



**Scheme 19** Han's preparation of secondary and tertiary phosphine oxides from menthyl *H*-phosphinates.

ligand, which proved to be so successful in the Rh-catalysed enantioselective hydrogenation of olefins (see above).<sup>33</sup>

However, efforts directed towards preparing enantiomerically pure secondary phosphine oxides – which, after deprotonation, offer a versatile synthon that reacts with a broad range of electrophiles – remained limited,<sup>77</sup> possibly due to the belief that the deprotonated secondary phosphine oxide anion is inherently stereolabile.<sup>78</sup>

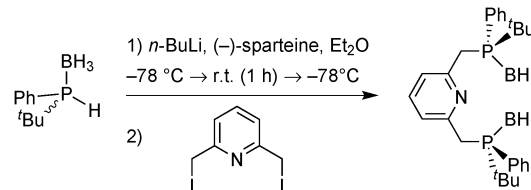
This prejudice was overturned by Han. In 2008, he reported that the rapid epimerization of (–)-menthyl (*R<sub>P</sub>*)-phenylphosphinate and its substitution products under alkaline conditions is not due to the stereolability of the secondary phosphine oxide anion, but originates from the reaction of the phosphinate ester with a metal alkoxide or hydroxide.<sup>68</sup> Thus, by carefully ensuring that no hydroxide or alkoxide is formed under the reaction conditions (*e.g.* with a menthol-free starting material), he prepared a variety of secondary and tertiary phosphine oxides with excellent enantiospecificity (Scheme 19).

The method has been applied, for example, in the preparation of organocatalysts for the Morita–Baylis–Hillman reaction<sup>79</sup> and of P-stereogenic macrocyclic N<sub>2</sub>P<sub>2</sub> ligands.<sup>80</sup> It is most successful when one of the substituents in the target (tertiary) phosphine is an aryl group, and is thus often an alternative to the Jugé–Stephan method. Also, menthol is cheap and readily available, and the reaction is easily scaled up. One drawback is the use of a phosphine oxide as the protecting group, though. Although a wealth of literature exists on the (stereospecific) reduction of secondary and tertiary phosphine oxides,<sup>81</sup> the reduction conditions need to be tuned to the specific system and are less general than for the deprotection of phosphine boranes.

## P\* pincer catalysts of metals other than iron

### PNP catalysts

The first PNP pincer ligands based on the pyridine backbone were prepared nearly 20 years ago (Scheme 21), and have found little attention since then. Zhang used Jugé's protocol<sup>65</sup> for his P(*o*-An)Ph-based ligand, which gave moderate enantioselectivity in the palladium-catalysed allylic alkylation and ruthenium-catalysed hydrosilylation.<sup>82</sup> Inspired by Evans' enantioselective



**Scheme 20** Livinghouse's P\* pincer synthesis by dynamic resolution/bisalkylation.

deprotonation,<sup>66</sup> Livinghouse developed a dynamic resolution/alkylation of the secondary *tert*-butylphenylphosphine borane to prepare the corresponding PNP pincer (Scheme 20).<sup>83</sup> Castillon applied this ligand in the ruthenium-catalysed hydrogenation of ketones with moderate to good enantioselectivity (60–95% ee at –40 °C).<sup>84</sup>

Imamoto prepared the P(<sup>*t*</sup>Bu)Me analogue and used it in a variety of enantioselective reactions.<sup>85</sup> These encompass Pd-catalysed Michael additions (1 out of 19 substrates gave >90% ee)<sup>85b</sup> and intramolecular hydroamination (up to 47% ee),<sup>85e</sup> Ir-promoted ketone hydrogenation (17% ee),<sup>85c</sup> and aza-Michael addition with a Ni catalyst (up to 46% ee).<sup>85d</sup>

### PCP catalysts

The first P-stereogenic PCP ligand, 1,3-bis(*tert*-butylphenylphosphinomethyl)benzene,<sup>86</sup> prepared in 2001 by van Koten with the dynamic resolution/alkylation protocol,<sup>83</sup> gave 18% ee in the Ru-catalysed ATH of acetophenone.<sup>86c</sup> More recently, Imamoto used enantiomerically pure *tert*-butylmethylphosphine borane to obtain the P(<sup>*t*</sup>Bu)Me analogue, which gave moderate enantioselectivity (up to 83% ee) in the Pd-catalysed addition of diarylphosphines to nitroalkenes.<sup>87</sup> The application in asymmetric catalysis of these PNP and PCP pincer ligands is discussed below in the context of our results with iron(II).

## P\* pincer catalysts of iron(II)

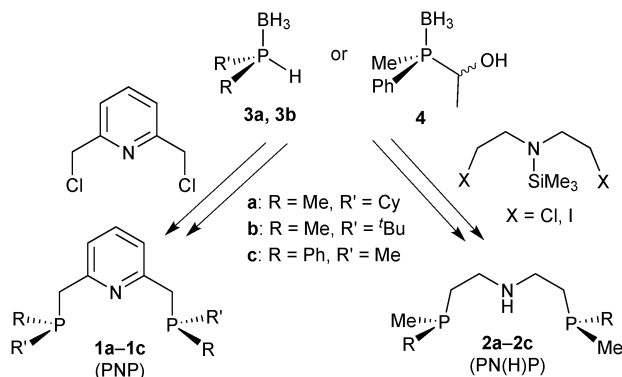
### Ligand scope and synthons

For our studies, we chose either the 2,6-dimethylpyridine (PNP, **1**)<sup>88,89</sup> or diethylamine backbones (PN(H)P, **2**)<sup>90</sup> in combination with P(Cy)Me (**a**), P(<sup>*t*</sup>Bu)Me (**b**), and P(Ph)Me (**c**) as P-stereogenic donors (Scheme 21).

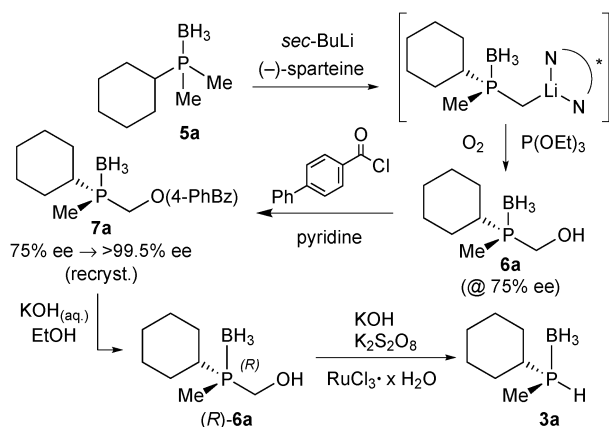
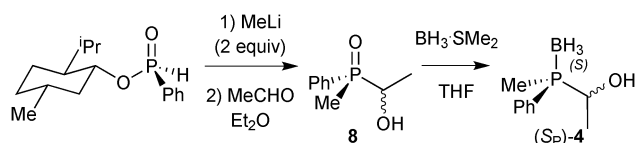
Enantiomerically pure *tert*-butylmethylphosphine borane (**3b**) was prepared by Imamoto's procedure (Scheme 17). As the iron(II) complexes of the P(<sup>*t*</sup>Bu)Me based pincer **1b** turned out to be unstable (see below), we also targeted its P(Cy)Me analogue **3a**. Imamoto's method gives (*R*)-cyclohexyl(hydroxymethyl)methylphosphine borane (**5a**) with 75% ee only, though.<sup>67</sup> Conversion of **5a** to the crystalline *p*-phenylbenzoyl ester and crystallisation gave **7a** as a single enantiomer. Thus, enantiomerically pure cyclohexylmethylphosphine borane (*R*)-**3a** was obtained after saponification and Ru-catalysed oxidation (Scheme 22).<sup>88</sup>

Finally, DFT calculations (see below) prompted us to prepare the P(Me)Ph-based pincers **1c** and **2c**. In this case, Imamoto's approach in Scheme 17 is not suitable, as methylphenylphosphine





Scheme 21 General synthetic pathway to the P-stereogenic pincers.

Scheme 22 Synthesis of enantiomerically pure (S)-cyclohexylmethylphosphine borane **7a**.Scheme 23 Preparation of masked secondary phosphine borane (*S<sub>P</sub>*)-**4** from (*R<sub>P</sub>*)-menthyl phenylphosphinate.

borane cannot be prepared as in Scheme 23 because the intermediate of type **6** undergoes overoxidation to the corresponding phosphinite borane  $\text{P}(\text{Me})(\text{Ph})(\text{OH})\cdot\text{BH}_3$ .<sup>67</sup> Also, methylphenylphosphide borane has been found to be configurationally unstable.<sup>91</sup> Therefore, we developed an alternative approach inspired by Buono's masked secondary phosphine boranes (**4**);<sup>92</sup> we treated diastereomerically pure (*R<sub>P</sub>*)-(-)-menthyl-*H*-phenylphosphinate (prepared on a multi-gram scale from (-)-menthol and  $\text{PhPCl}_2$ )<sup>93</sup> with MeLi, quenched the lithium salt of the methylphenylphosphine oxide with acetaldehyde, and reduced (*S<sub>P</sub>*)-(1-hydroxyethyl)methylphenylphosphine oxide **8** with  $\text{BH}_3\cdot\text{SMe}_2$  to (*S<sub>P</sub>*)-(1-hydroxyethyl)methylphenylphosphine borane (**4**) with formal retention (Scheme 23).<sup>94</sup> This route is easily scalable, and (*S<sub>P</sub>*)-**4** was routinely prepared on a >5 g scale.<sup>89</sup>

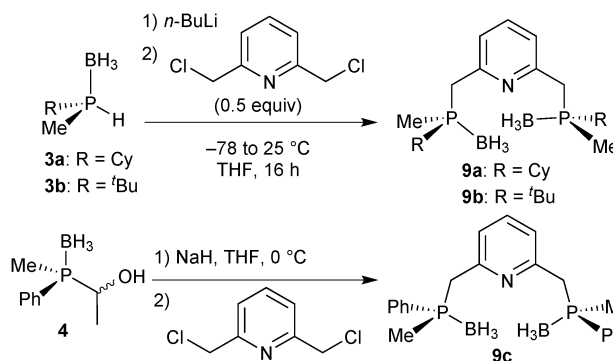
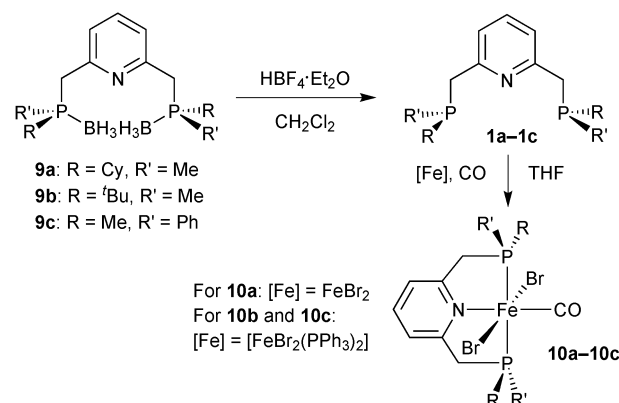
## Pyridine based pincer complexes

### PNP ligand synthesis

The  $\text{P}(\text{Me})\text{R}\cdot\text{BH}_3$  ( $\text{R} = \text{Cy}$ , **3a**;  $\text{R} = t\text{-Bu}$ , **3b**) units were installed onto the 2,6-dimethylpyridine backbone to give the borane-protected PNP pincer ligands **9a** and **9b** following Imamoto's procedure (Scheme 24).<sup>85a</sup> The phenylmethylphosphine pincer **9c** was prepared by base induced deacylation of **4**, followed by double alkylation with 2,6-bis(chloromethyl)pyridine.<sup>89</sup> Ligand **9c** has been previously prepared by a different procedure on a small scale (<50 mg) as a 58:42 *C*<sub>2</sub>:*meso* diastereomeric mixture (84% ee for the *C*<sub>2</sub> diastereomer).<sup>95</sup>

### [FeBr<sub>2</sub>(CO)(PNP)]

The borane adducts **9a–9c** were deprotected with  $\text{HBF}_4\cdot\text{OEt}_2$  in dichloromethane<sup>72</sup> to the free pincer ligands **1a–1c**, which were treated with a suitable iron source ( $\text{FeBr}_2$  or  $[\text{FeBr}_2(\text{PPh}_3)_2]$ ) under a CO atmosphere to give the iron dibromocarbonyl complexes *mer,trans*- $[\text{FeBr}_2(\text{CO})(\text{1a–1c})]$  (**10a–10c**) (Scheme 25).<sup>88</sup> These complexes are typically deep blue, whereas the *cis* dibromo analogues are red (see below). Complexes **10a–10c** are stable towards air and moisture. In the work-up, **10a** is washed with water in air. However, the stability of **10a–10c** decreases with increasing steric bulk of the substituents on phosphorus. Thus, the *tert*-butylmethylphosphine derived complex **2b** slowly decomposes both in solution and in the solid state.

Scheme 24 Preparation of borane-protected PNP pincer ligands **9a–9c**.Scheme 25 Preparation of iron dibromocarbonyl complexes **2a–2c**.



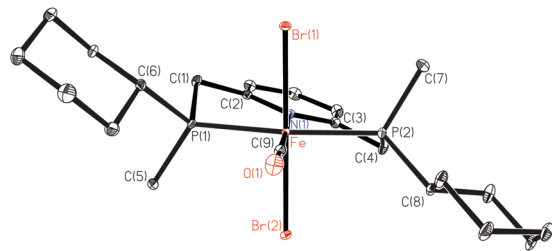


Fig. 1 ORTEP drawing of **10a** (reprinted with permission from ref. 88. Copyright 2018 American Chemical Society).

The X-ray structure of **10a** (Fig. 1) reveals that the pyridine-pincer backbone of **1a** is tilted to enable the envelope conformation for the two chelate rings.<sup>88</sup>

Depending on the stereocentre at phosphorus, the tilt is either  $\lambda$  (as for **10a** with (*S,S*)-**1a**) or  $\delta$  (observed for **10c** with (*R,R*)-**1c**), and the large substituent on phosphorus occupies a pseudo-equatorial position.

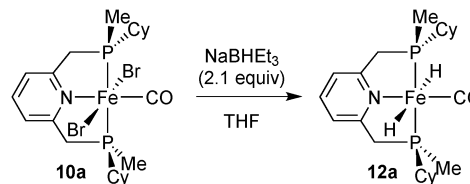
### Hydride complexes

The dibromocarbonyl complexes **10a–10c** react with NaBHET<sub>3</sub> (1 equiv.) in THF or CH<sub>2</sub>Cl<sub>2</sub> to give the bromohydridocarbonyl complexes [FeBrH(CO)(PNP)] (**11a–11c**) (Scheme 26). In the major isomer of **11a–11c**, the hydride ligand is located *trans* to bromide.

All hydrides are extremely sensitive towards air and moisture, and the P(<sup>*t*</sup>Bu)Me derivative **11b** was not isolable in reasonable purity. As hydrides **11b–11c** decompose in solution, they were always freshly prepared for catalytic experiments. A putative decomposition product (among unidentified brown precipitates) is an iron(0) dicarbonyl complex, as observed for Fe complexes of the achiral 2,6-bis(diisopropylphosphinomethyl)pyridine pincer.<sup>16</sup> As for dibromocarbonyl complexes, bulkier phosphines (e.g. *tert*-butyl substituted ones) form less stable complexes.

Due to its potential role in catalysis (see below), we also prepared dihydride **12a** (Scheme 27). The major species contains *trans* hydrides, but the other components of the reaction mixture were not characterised. The dihydride is highly sensitive towards air and moisture and decomposes in solution.

Addition of a stoichiometric amount of acetophenone to **12a** did not change the major species present in a C<sub>6</sub>D<sub>6</sub> solution as observed by NMR spectroscopy, and only trace amounts (<2%) of phenylethanol were formed (which might originate from impurities of **12a**). A similar observation has been made for an



Scheme 27 Preparation of iron dihydridocarbonyl complex **12a**.

achiral Fe/PNP dihydride.<sup>96</sup> This indicates that the dihydride **12a** is not involved in the catalytic cycle of ketone hydrogenation with such complexes.

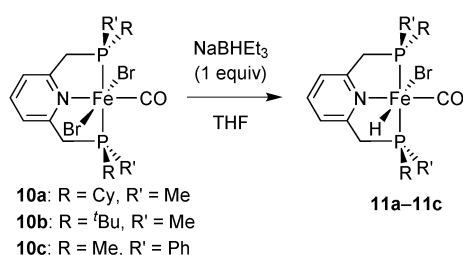
### Hydrides **11a–11c** in asymmetric hydrogenation

After dehydrobromination with base (KO<sup>*t*</sup>Bu), the hydride complexes **11a–11c** catalyse the hydrogenation of ketones under H<sub>2</sub> pressure.<sup>88</sup> The best results obtained for acetophenone (**13**) as a model substrate are given in Scheme 28. Under optimised conditions, catalyst **11a** achieved full conversion of **13** to (*S*)-1-phenylethanol (**14**). The *tert*-butylmethylphosphine derived complex **11b** and phenylmethylphosphine derived **11c** gave lower conversion (70 and 28%, respectively). Overall, the enantioselectivity was modest and reached 48% ee with the cyclohexylmethylphosphine derived pincer **11a**.

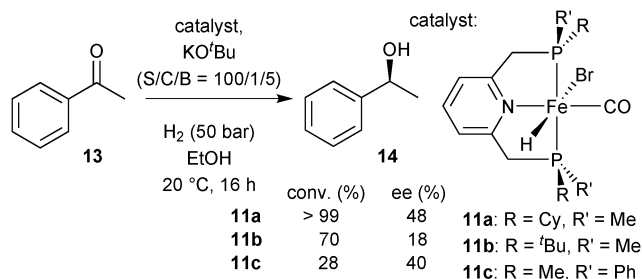
### DFT study on [FeHBr(CO)(**1a**)], **11a**

To improve the ligand design, we were confronted with the need for a stereochemical model for enantiodiscrimination. This involved us in a long-standing mechanistic dispute concerning the related achiral P(<sup>*t*</sup>Bu)<sub>2</sub> based iron(II) catalyst for ketone hydrogenation,<sup>16</sup> for which different mechanisms have been studied (Scheme 29). Milstein's original suggestion of an inner sphere mechanism (I)<sup>16</sup> has been challenged by Yang and Hopmann, who proposed outer sphere mechanisms of type D based on a dihydride complex (**12**).<sup>96</sup>

Eventually, Milstein put forward the outer-sphere mechanism O, which involves the iron(0) species **15** whose chiral analogue is shown in Scheme 30.<sup>97</sup> The base dehydrobrominates precatalyst **11a** to give a dearomatised intermediate that reductively eliminates H<sup>+</sup>. Rearomatisation and EtOH coordination give the iron(0) species **15**, which then transfers a benzylic H atom from the PNP ligand as hydride to the carbonyl group of acetophenone (Scheme 30, D). A hydrogen bond involving the coordinated ethanol molecule directs the incoming substrate and

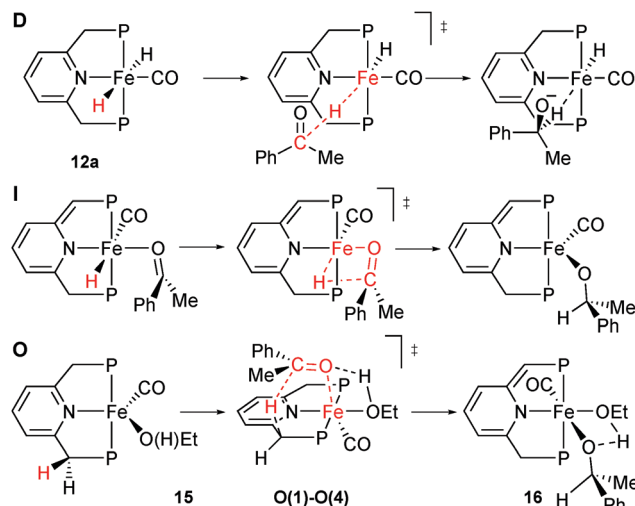


Scheme 26 Synthesis of hydrides **11a–11c**.



Scheme 28 Acetophenone hydrogenation with **11a–11c** as catalysts.





Scheme 29 Proposed mechanisms for the hydrogenation of ketones with **11a**.

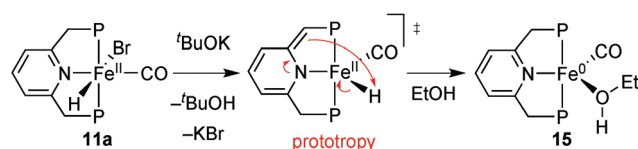
activates its carbonyl group towards nucleophilic attack, which is reminiscent of the well-established bifunctional mechanism.<sup>23</sup>

We reasoned that the additional stereochemical information provided by the chiral ligand may help discriminate between these mechanisms, and hence undertook a comprehensive DFT study by modelling the enantiodetermining steps of the three mechanisms in Scheme 30.<sup>88</sup> Notably, only the outer-sphere mechanism **D** predicts the experimental sense of induction and the enantioselectivity, in agreement with Milstein's proposal which is mostly based on kinetic considerations.<sup>97</sup> Beyond contributing to assess the mechanism, the DFT study revealed the conformational issues discussed below.

### Pincer ligand conformation

The X-ray structure of dibromocarbonyl **10a** shows that the 5-membered rings P(1)–Fe–N(1)–C(2)–C(1) and P(2)–Fe–N(1)–C(3)–C(4) assume envelope conformations with the P atoms in the *endo* position and equatorial cyclohexyl groups (Fig. 1). The torsion angles P(1)–Fe–N(1)–C(2) ( $\theta_1$ ) and P(2)–Fe–N(1)–C(3) ( $\theta_2$ ) describe the conformation of the five-membered chelate rings in the iron-bound PNP pincer (Fig. 2).

The conformation of the chelate ring determines the position of the P-substituents (equatorial or axial in the envelope conformation or inclinal in the planar one)<sup>32b</sup> and the tilt of the pyridine ring with respect to the Fe/PNP plane. The inversion of the ring swaps the cyclohexyl and methyl P substituents between equatorial and axial positions and tilts the pyridine ring with respect to the P(1)–Fe–N(1) and P(2)–Fe–N(1) planes.



Scheme 30 Formation of the iron(0) species **15** from **11a**.

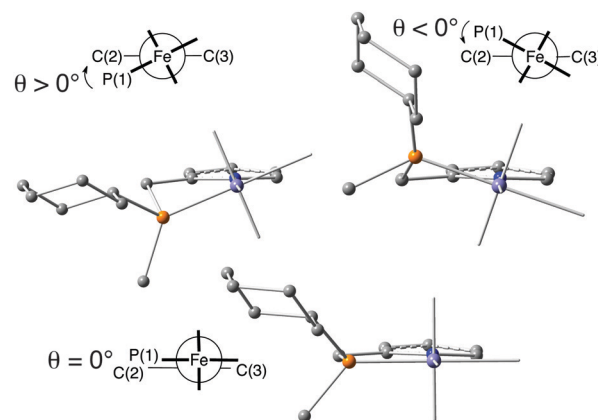


Fig. 2 Conformation of the five-membered chelate ring (with Newman projection and dihedral angle  $\theta$ ) (reprinted with permission from ref. 88. Copyright 2018 American Chemical Society).

Positive torsion angles ( $\theta_1$  and  $\theta_2$ ) correspond to equatorial cyclohexyl groups and to the  $\lambda$  conformation of the backbone. For negative  $\theta$  values ( $-12^\circ$  to  $-27^\circ$ ), the cyclohexyl is axial, and the backbone is in the  $\delta$  conformation. The calculations indicate that the five-membered chelate ring can also assume a planar conformation ( $\theta$  close to  $0^\circ$ ) with inclinal substituents.

In the enantiodetermining step of Milstein's unprecedented outer-sphere mechanism **O**, a benzylic H atom of the ligand is transferred as hydride from the five-coordinate iron(0) complex [Fe(CO)(EtOH)(**1a**)] (**15**) to acetophenone (Scheme 30 **O**). Complex **15** exists in two different conformations of the chelate ring (**15a** and **15b**). The approaching acetophenone is directed by the incipient C=O...Fe interaction and by the C=O...HOEt hydrogen bond to the ethanol ligand. As acetophenone approaches the iron(0) complex **15a/15b**, the conformation of the chelate ring changes to allow the attack of the benzylic H atom as hydride onto the carbonyl C atom (Fig. 3). The conformation determines from which benzylic position the hydride is transferred, and acetophenone approaches with either enantioface, for a total of four transition states, **O(1)–O(4)**. Intriguingly, the most stable TS **O(1)** features axial cyclohexyl groups and hence the less stable conformation.

The intrinsic reaction coordinate (IRC) analysis shows that **O(2)** and **O(4)** connect to **15a**, which bears equatorial cyclohexyl groups, whereas **O(1)** and **O(3)** are linked to **15b**, which bears axial cyclohexyl groups. Also, conformer **15a**, which bears equatorial cyclohexyl substituents, converts to **15b**, which is less stable by 0.4 kcal mol<sup>-1</sup>.

Conformers **15a** and **15b** interconvert rapidly and react under Curtin–Hammett conditions to give the 1-phenylethoxide complexes **16a/16a'** and **16b/16b'** (Fig. 4). This implies that the ratio of the products depends on the energy difference between the transition states.<sup>98</sup>

The small changes in  $|\theta|$  (Fig. 3) indicate minor structural reorganization between the Fe(0) species **15a/15b** and **O(1)–O(4)**, which further supports the retention of conformation along the reaction coordinate. Conformer **15b** (with axial cyclohexyl groups)



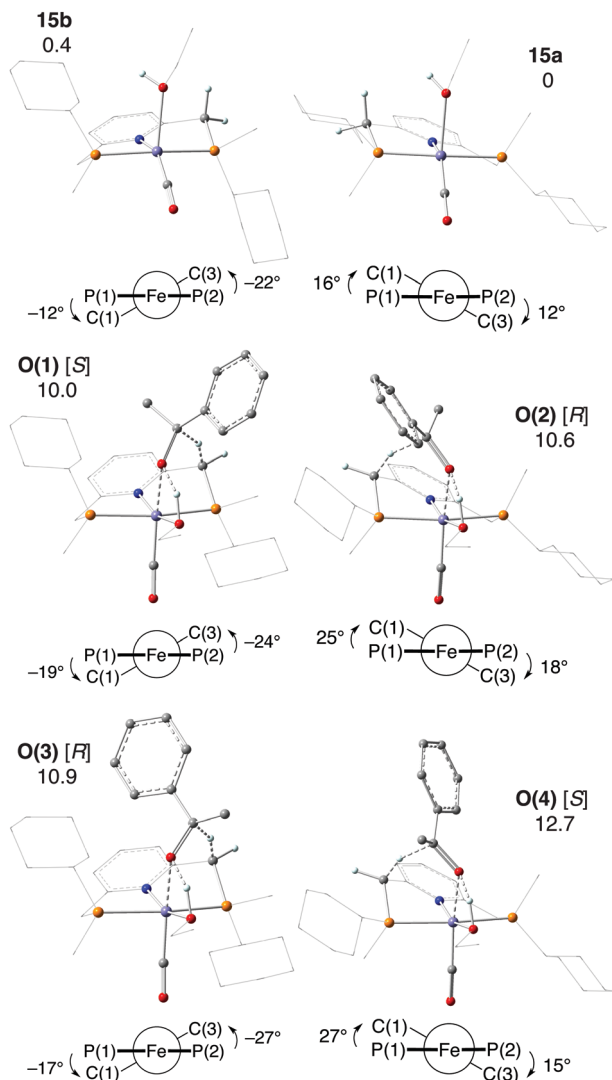


Fig. 3 Iron(0) complexes **15a** and **15b** and TSs **O(1)**–**O(4)** for hydride transfer in mechanism **O** (product stereochemistry in brackets). Newman projections give  $\theta_1$  (left) and  $\theta_2$  (right). Relative Gibbs free energies are in kcal mol<sup>−1</sup> (reprinted with permission from ref. 88. Copyright 2018 American Chemical Society).

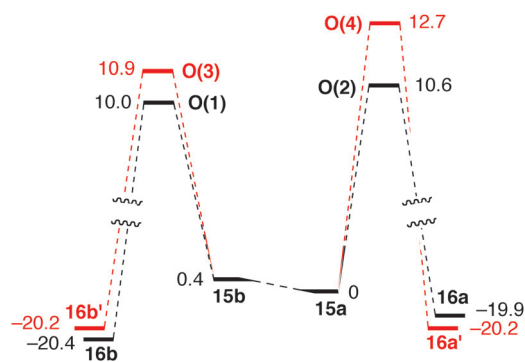


Fig. 4 Reaction pathway for H<sup>−</sup> transfer in mechanism **O**. Relative Gibbs free energies are in kcal mol<sup>−1</sup> (reprinted with permission from ref. 88. Copyright 2018 American Chemical Society).

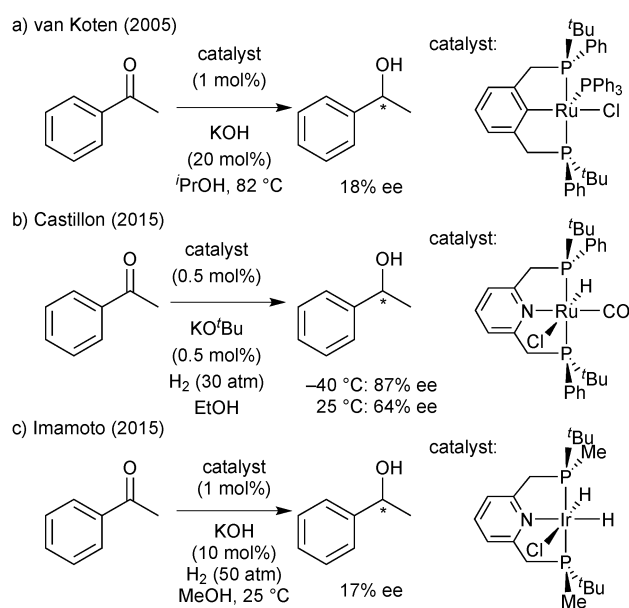
is just 0.4 kcal mol<sup>−1</sup> less stable than **15a**, which bears equatorial cyclohexyls. The major contribution to the total energy of the **O(1)**–**O(4)** transition states is the distortion of the catalyst, *i.e.* the conformational change of the chelate ring involved in hydride transfer. However, the energetic preference for conformations in which the large P-substituents occupy equatorial positions is small, and can be reversed as the substrate approaches. Even weak intermolecular interactions, such as C–H⋯O or C–H⋯ $\pi$ , swap the relative stability of the conformations of different intermediates and transition states. Therefore, it is reasonable to assume that the conformational flexibility observed for **1a** might be a more general problem with P-stereogenic pincer ligands with a pyridine backbone (see below).

### Comparison with other P-stereogenic PNP/PCP ligands

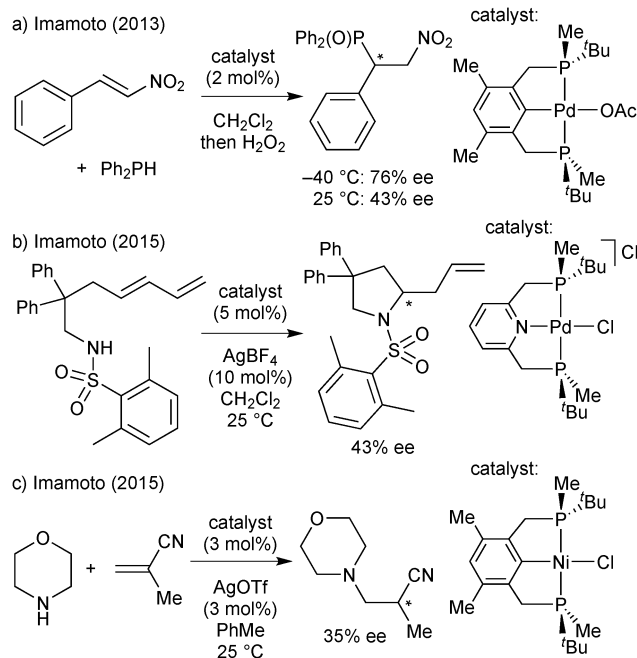
PNP and PCP ligands similar to ligand **1a** have been studied for their application in hydrogenation (Scheme 31)<sup>84,85c,86c</sup> and hydrophosphination/hydroamination (Scheme 32).<sup>85b,d,e,87</sup>

Overall, the enantioselectivity was modest and/or strongly temperature dependent. In the ruthenium-catalysed ketone hydrogenation of ketones, the reduction of acetophenone was much more enantioselective at −40 than at 25 °C (87 and 64% ee, respectively, Scheme 31b).<sup>84</sup> Palladium-catalysed hydrophosphinations show similar effects of the temperature (Scheme 32a, ref. 85b gives a further example).<sup>85b,87</sup>

Conformational equilibria of the 2,6-dimethylenepyridine (PNP) or 1,3-xylyl (PCP) backbones analogous to those described above for **11a** may account for these temperature effects, but a conformational analysis would be needed to verify this hypothesis. Still, our observations with the PNP pincer ligand **1a** prompted us to move to PN(H)P ligands with *N,N*-diethyleneamine as a backbone, in which the sp<sup>3</sup> nitrogen atom should act as a conformational lock upon coordination to a metal centre.



Scheme 31 PNP/PCP ligands in hydrogenation reactions.



Scheme 32 PNP/PCP ligands in hydrophosphination and hydroamination reactions.

## PN(H)P pincer complexes

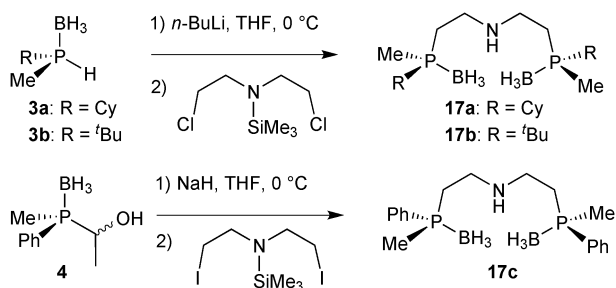
### Synthesis of PN(H)P pincers

As for their PNP analogues, we prepared the borane-protected PN(H)P pincer ligands **17a–17c** by deprotection of **3a** and **3b** and subsequent alkylation with bis(2-chloroethyl)-*N*-trimethylsilylamine (Scheme 33).<sup>90</sup>

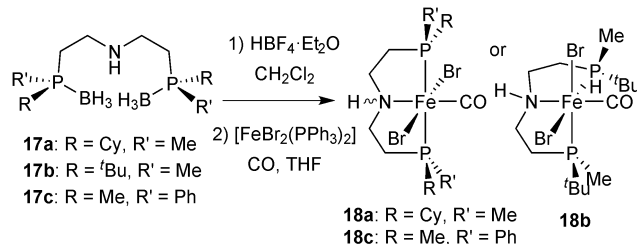
The phenylmethylphosphine derived pincer **17c** was prepared from the masked secondary phosphine borane **4** and bis(2-iodoethyl)-*N*-trimethylsilylamine (analogously to **9c**). The borane-protected pincer ligands **17a–17c** are indefinitely stable upon storage in air at room temperature.

### [FeBr<sub>2</sub>(CO)(PN(H)P)]

After deprotection of **17a–17c** with HBF<sub>4</sub>·OEt<sub>2</sub> in dichloromethane,<sup>72</sup> pincers **2a–2c** form the dibromocarbonyl complexes [FeBr<sub>2</sub>(CO)(**2a–2c**)] (**18a–18c**) by reaction with [FeBr<sub>2</sub>(PPh<sub>3</sub>)<sub>2</sub>] under a CO atmosphere (Scheme 34). Complexes **18a** and **18c** are blue with a meridional pincer ligand and mutually *trans*



Scheme 33 Alkylation of secondary phosphine boranes to give the protected PN(H)P pincers.



Scheme 34 Synthesis of dibromocarbonyl complexes **5a–5c**.

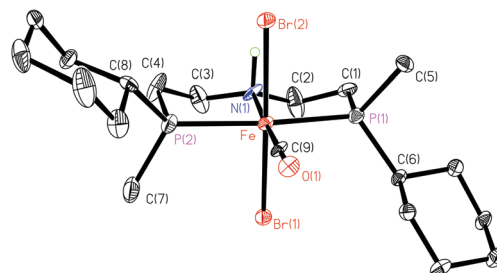


Fig. 5 ORTEP drawing of **18a** (reprinted with permission from ref. 90).

bromides, whereas the *tert*-butylmethylphosphine-derivative **5b** is red with facial pincer and *cis* bromides.

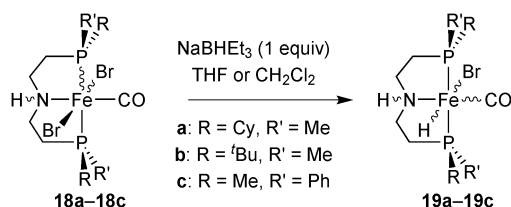
Overall, the PN(H)P pincer ligands **2a–2c** form iron complexes that are less stable than those with the pyridine backbone (**1a–1c**). Hence, complexes **18a–18c** are best handled under an inert atmosphere, although brief exposure to ambient conditions is tolerated. In particular, the *tert*-butylmethylphosphine derivative **18b** is unstable and slowly decomposes both in solution and in the solid state.

The conformation of the chelate rings with the *N,N*-diethylamine backbone is rigidified by the sp<sup>3</sup> nitrogen (Fig. 5). The metallacycles adopt an envelope conformation with C(2) and C(3) in the *endo* position, and the elongated ellipsoids of the backbone indicate the presence of an isomeric form where the N–H proton points downwards, leading to a ring flip.

### Hydride complexes

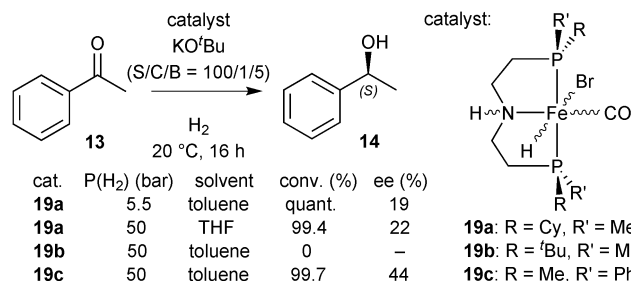
Treatment of the dibromocarbonyl complexes **18a–18c** with NaBHET<sub>3</sub> (1 equiv.) in THF or CH<sub>2</sub>Cl<sub>2</sub> gave the bromohydrido-carbonyl derivatives **19a–19c** (Scheme 35).

The hydride ligand is located *trans* to bromide in the major isomer of hydride **19a** and *trans* to CO in **19b** and **19c**. Hydrides **19a–19c** are extremely sensitive towards air and moisture.



Scheme 35 Synthesis of PN(H)P bromohydrido-carbonyl complexes.



Scheme 36 Asymmetric hydrogenation of acetophenone with **19a–19c**.

As they decompose in solution, they were freshly prepared for each catalytic run.

### Hydrides **19a–19c** as catalysts

In a preliminary screening, we tested hydrides **19a** and **19b** in the hydrogenation of acetophenone (**13**) after dehydrobromination.<sup>90</sup> The P(Cy)Me analogue **19a** gave the best activity in toluene (quantitative conversion after 16 h at 5.5 bar H<sub>2</sub>), but with low enantioselectivity (19% ee), and the P(<sup>t</sup>Bu)Me derivative **19b** was not active (Scheme 36).<sup>90</sup>

### Origin of enantioselectivity with Fe/PN(H)P catalysts

To explain the low enantioselectivity of **19a** and improve the ligand design, we used DFT calculations to model the enantiodetermining hydride transfer step **TS20a**, assuming the same mechanism as the achiral [FeBrH(CO)(<sup>t</sup>Pr<sub>2</sub>P(CH<sub>2</sub>)<sub>2</sub>N(H)(CH<sub>2</sub>)<sub>2</sub>P<sup>t</sup>Pr<sub>2</sub>)]<sup>21b</sup> (Scheme 37).

The diastereoisomeric transition states **TS20aS** and **TS20aR** lead to (*S*)- and (*R*)-1-phenylethanol, respectively (Fig. 6 top). The calculated energy difference (0.5 kcal mol<sup>−1</sup>, hybrid DFT model at the B3LYP level of theory) is in fair agreement with the experimental one (*ca.* 0.2 kcal mol<sup>−1</sup>).

We speculated that the low energy difference between **TS20aS** and **TS20aR** may result from the occurrence of a similar CH/π interaction with the phenyl group of acetophenone in both transition states which involves the C<sub>ipso</sub>–H of the

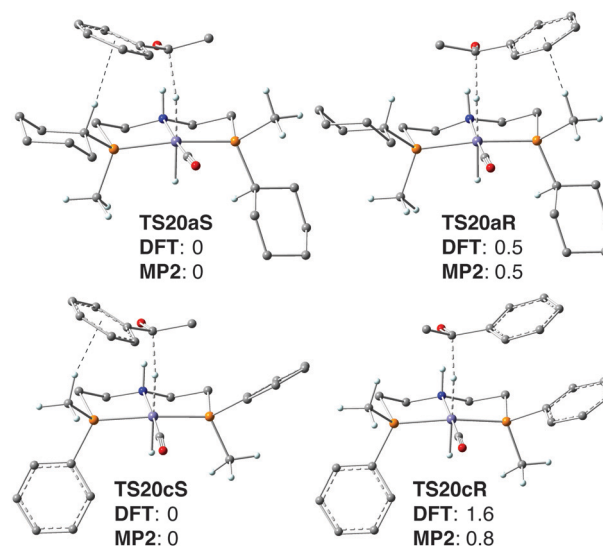
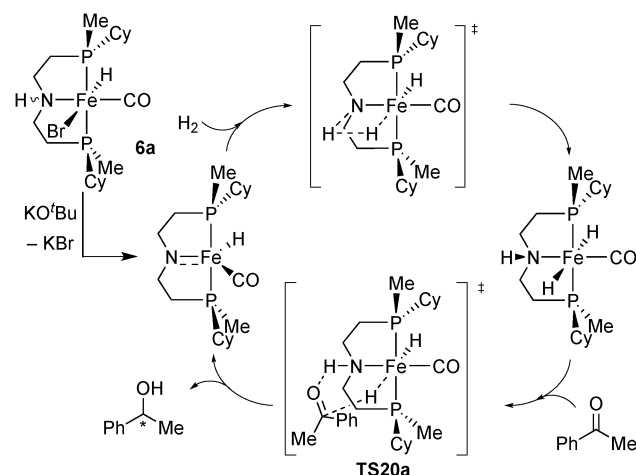


Fig. 6 Transition states **TS20a/cS** and **TS20a/cR** for the hydride transfer. Relative Gibbs free energies are in kcal mol<sup>−1</sup>. Black dashed lines depict the hydride transfer and the C–H...π interaction.

cyclohexyl in **TS20aS** and the methyl on phosphorus in **TS20aR** (Fig. 6 top) (in addition to a strong N–H...O hydrogen bond that directs and activates acetophenone). Therefore, we tried to increase the enantioselectivity by eliminating selectively one of CH/π interactions.

To this goal, the cyclohexyl group was replaced with a phenyl ring *in silico*, which eliminated the C–H...π interaction in transition state **TS20cR** (Fig. 6 bottom). This gave an increased energy difference of 1.6 kcal mol<sup>−1</sup> between the diastereoisomeric TSs **TS20cS** and **TS20cR**, which corresponds to 88% ee. These computational results motivated us to tackle the synthetic challenge of introducing an enantiomerically pure phenylmethylphosphine unit onto the backbone (a primary alkyl halide) and prepare the new pincer ligand **2c** as described above.

Disappointingly, however, the phenylmethylphosphine-derived bromocarbonylhydride complex [FeBrH(CO)(**2c**)] (**19c**) gave only 44% ee (Scheme 36), which implies an energy difference for the enantiodetermining transition states of 0.6 kcal mol<sup>−1</sup>. Surprised at first, we tested other DFT functionals and basis sets, but all gave energy values within ±0.4 kcal mol<sup>−1</sup> of 1.6 kcal mol<sup>−1</sup>. Eventually, single-point energy calculations with MP2 gave an energy difference of 0.6 kcal mol<sup>−1</sup> between **TS20cS** and **TS20cR** (Fig. 6 bottom), which perfectly corresponds to the experimental enantioselectivity of 44% ee. Most probably, DFT fails to predict the enantioselectivity accurately with the P(Me)Ph-based pincer **2c** because it overestimates the energy of the C–H...π interactions, which is a known effect.<sup>90</sup> When the diastereoisomeric TSs contain the same number of CH/π interactions (such as **TS20aS** and **TS20aR**, which have one each, Fig. 6), the errors cancel out, and DFT and MP2 give the same result. Instead, for **2c**, only the less energetic **TS20cS** features a CH/π interaction whose energy is most probably overestimated by DFT, leading to a spuriously high energy difference with **TS20cR** (1.6 kcal mol<sup>−1</sup>, vs. 0.8 kcal mol<sup>−1</sup> by MP2).

Scheme 37 Proposed mechanism for the hydrogenation of ketones with Fe/PN(H)P catalyst **31a**.

A further intriguing feature is that, although catalysts **19a** and **19c** contain pincer ligands with opposite P-stereochemistry (*S* vs. *R*, respectively) they hydrogenate acetophenone with the same sense of induction (*S*). Therefore, the methyl group acts as the “small” substituent with PMe(Ph) (**TS20c**), but as the “large” one with P(Cy)Me (**TS20a**) (Fig. 6), which suggests that attractive non-covalent interactions (NCI, *e.g.* CH/ $\pi$ ,  $\pi/\pi$  stacking), rather than repulsive steric hindrance, dominate (or at least strongly influence) enantioselection with these ligands, which are not exceedingly bulky. The NCI analysis supports this view.<sup>90</sup> Interestingly, similar observations have been made with P-stereogenic diphosphines in the context of the quadrant rule. Gridnev has identified attractive interactions (C–H/ $\pi$  or C–H/H–C) between the coordinated substrate and the ligand even in the crowded quadrants. Increasing the overall steric bulk tightens the contacts and turns attraction to repulsion.<sup>35b</sup>

The importance of non-covalent interactions poses a further challenge to the rational ligand design by calculation. In particular, hybrid DFT methods, although a reliable tool to study the geometry of transition states, do not deliver energy values that are accurate enough to predict the enantioselectivity when weak interactions (such as C–H $\cdots\pi$ ) are involved. Post Hartree–Fock methods such as MP2 are more accurate, but much more demanding computationally than hybrid DFT methods.

## Conclusions and outlook

### Differences between dialkyl- and diarylphosphine donors

When we started our study of P-stereogenic pincer ligands some years back, we chose dialkylphosphine donors by analogy with the existing achiral PNP pincer complexes of iron(II). In particular, the combination of methyl with a bulky group such as *tert*-butyl or cyclohexyl, as in Imamoto's approach, seemed promising. In retrospect, we recognise now that PR<sub>2</sub> based ligands are more difficult to design than those based on PAR<sub>2</sub> donors (R = alkyl, Ar = aryl). The above sections have shown that conformational issues are (literally) pivotal in P-stereogenic pincer ligands as well as in bidentate ones.

Thus, in P-stereogenic diphosphines, the substituents of phosphorus must differ largely in size to lock the chelate in the conformation in which the large substituent occupies the equatorial position. As aryl substituents on phosphorus are flat, their apparent size depends on their conformation. Hence, in DiPAMP, the axial phenyl group acts as the small substituent with respect to the chelate, but as the large substituent toward the substrate (Scheme 6). With P(<sup>*t*</sup>Bu)Me (or P(Cy)Me) as donors, instead, the large substituent occupies the equatorial position, leaving the small methyl group axial. In this conformation, both substituents act as small, notwithstanding from which direction the substrate approaches. This is illustrated by the crystal structure of **18a** (Fig. 5) and in the transition state **TS20aS** (Fig. 6). Therefore, one might speculate that methyl as the axial group is too small to enforce strong enantiodiscrimination. In fact, the situation is more complex, as our studies with the PNP and PN(H) pincers show.

### Overall steric bulk and attractive interactions

We have found that, in the enantiodetermining transition states, the PNP pincer ligand with P(Cy)Me donors (**1a**) can favour the conformation that features axial cyclohexyl groups (Fig. 3). This obviously results from the flexibility of the backbone that allows for the axial/equatorial switch, but also suggests that the overall steric bulk on the pincer is not very large (otherwise the axial cyclohexyl would cost too much energy), at least in outer sphere reactions as those studied here. The modest enantioselectivity achieved with the conformationally rigid PN(H)P pincer with P(Ph)Me donors (**2c**, Scheme 36) supports the view that methyl-containing P-stereogenic units do not offer adequate steric bulk. In this context, the DFT study with the PN(H)P pincer ligand **2c** indicates that attractive interactions play a major role in enantiodiscrimination. This may be seen as an indication that, when steric repulsions are moderate, attractive non-covalent interactions also play a significant role in enantiodiscrimination as already discussed for P-stereogenic diphosphines.<sup>35b</sup> We recognise that our understanding of the mechanisms of chirality transfer is, even after so many decades, still fragmentary and incomplete. DFT studies are increasingly important in this respect, but their accuracy in the descriptions of weak interactions needs improvement before rational ligand design by calculation becomes reality in asymmetric catalysis.

### Outlook

Overall, the topic of this article is the use of stereogenic phosphorus to control the conformation of a chelate, be it in a bidentate or in a tridentate ligand. We have discussed the pitfalls of this approach at length, and concluded that a rigid backbone should be used in such ligands. Obviously, the straightforward method to solve it is to incorporate a stereo-centre in the backbone. This does not necessarily mean that purely P-stereogenic pincer ligands have little chance of success, though, and does not relegate stereogenic phosphorus to a mere supporting role. In particular, the combination of P-stereogenic diarylphosphine units (PARAr') with dialkyl ones (even achiral such as PR<sub>2</sub>), which is unexplored yet, might increase the overall steric bulk and hence enantioface discrimination without decreasing significantly the stability of the catalyst. In fact, iron(II) complexes with mixed P<sup>i</sup>Pr/PPh<sub>2</sub> donors have been prepared and used in asymmetric hydrogenation (Scheme 2).<sup>26–28</sup>

Alternatively stereogenic phosphorus can be exploited to direct the configuration of multiple chelate rings of a polydentate ligand. In this case, the multichelate structure is the element of rigidity whose necessity has been recognised in the above discussion. With our N<sub>2</sub>P<sub>2</sub> macrocyclic ligands, we have shown that this approach generates extremely rigid structures with predictable structure and absolute configuration that deliver high enantioselectivity in the transfer hydrogenation of ketones for a broad substrate scope.<sup>10</sup> Therefore, we believe that stereogenic phosphorus will continue to play an important role in the synthesis and stereochemical understanding of asymmetric catalysis.



## Conflicts of interest

There are no conflicts to declare.

## Acknowledgements

The authors are grateful to ETH Zürich (grant ETH-36 17-1) and to the Swiss National Science Foundation (grant 200020-146881) for financial support.

## Notes and references

- (a) A. Grabulosa, *P-Stereogenic Ligands in Enantioselective Catalysis*, RSC Publishing, Cambridge, 2011; (b) M. Dutartre, J. Bayardon and S. Jugé, *Chem. Soc. Rev.*, 2016, **45**, 5771.
- Non-Noble Metal Catalysis: Molecular Approaches and Reactions*, ed. R. J. Klein Gebbink and M. C. Moret, Wiley-VCH, Weinheim, 2019.
- I. Bauer and H. J. Knölker, *Chem. Rev.*, 2015, **115**, 3170.
- A. Fürstner, *Angew. Chem., Int. Ed.*, 2009, **48**, 1364.
- The Handbook of Homogeneous Hydrogenation*, ed. J. G. de Vries and C. J. Elsevier, Wiley-VCH, Weinheim, 2007.
- H. U. Blaser, B. Pugin and F. Spindler, *Top. Organomet. Chem.*, 2012, **42**, 65.
- Seminal papers: (a) T. Ohkuma, H. Ooka, S. Hashiguchi, T. Ikariya and R. Noyori, *J. Am. Chem. Soc.*, 1995, **117**, 2675; (b) J. X. Gao, T. Ikariya and R. Noyori, *Organometallics*, 1996, **15**, 1087. For accounts of the evolution from ruthenium to iron, see: (c) R. H. Morris, *Chem. Rev.*, 2016, **16**, 2644; (d) R. H. Morris, *Dalton Trans.*, 2018, **47**, 10809.
- C. Sui-Seng, F. Freutel, A. J. Lough and R. H. Morris, *Angew. Chem., Int. Ed.*, 2008, **47**, 940.
- W. Zuo, A. J. Lough, Y. F. Liand and R. H. Morris, *Science*, 2013, **342**, 1080.
- Selected papers: (a) R. Bigler, R. Huber and A. Mezzetti, *Angew. Chem., Int. Ed.*, 2015, **54**, 5171; (b) L. De Luca and A. Mezzetti, *Angew. Chem., Int. Ed.*, 2017, **56**, 11949; (c) L. De Luca, A. Passera and A. Mezzetti, *J. Am. Chem. Soc.*, 2019, **141**, 2545.
- V. Rautenstrauch, X. Hoang-Cong, R. Churlaud, K. Abdur-Rashid and R. H. Morris, *Chem. – Eur. J.*, 2003, **9**, 4954.
- W. W. Zuo, S. Tauer, D. E. Prokopchuk and R. H. Morris, *Organometallics*, 2014, **33**, 5791.
- S. Werkmeister, J. Neumann, K. Junge and M. Beller, *Chem. – Eur. J.*, 2015, **21**, 12226.
- (a) T. Zell and D. Milstein, *Acc. Chem. Res.*, 2015, **48**, 1979; (b) K. L. Szabo and O. F. Wendt, *Pincer and Pincer-Type Complexes: Applications in Organic Synthesis and Catalysis*, Wiley-VCH, Weinheim, 2014.
- J. I. van der Vlugt and J. N. H. Reek, *Angew. Chem., Int. Ed.*, 2009, **48**, 8832.
- R. Langer, G. Leitun, Y. Ben-David and D. Milstein, *Angew. Chem., Int. Ed.*, 2011, **50**, 2120.
- T. Zell, Y. Ben-David and D. Milstein, *Catal. Sci. Technol.*, 2015, **5**, 822.
- J. A. Garg, S. Chakraborty, Y. Ben-David and D. Milstein, *Chem. Commun.*, 2016, **52**, 5285.
- T. Zell, Y. Ben-David and D. Milstein, *Angew. Chem., Int. Ed.*, 2014, **53**, 4685.
- N. Gorgas, B. Stöger, L. F. Veiros, E. Pittenauer, G. Allmaier and K. Kirchner, *Organometallics*, 2014, **33**, 6905.
- (a) S. Werkmeister, K. Junge, B. Wendt, E. Alberico, H. J. Jiao, W. Baumann, H. Junge, F. Gallou and M. Beller, *Angew. Chem., Int. Ed.*, 2014, **53**, 8722. See also: (b) H. Jiao, K. Junge, E. Alberico and M. Beller, *J. Comput. Chem.*, 2016, **37**, 168.
- S. Chakraborty, H. G. Dai, P. Bhattacharya, N. T. Fairweather, M. S. Gibson, J. A. Krause and H. R. Guan, *J. Am. Chem. Soc.*, 2014, **136**, 7869.
- (a) K. J. Haack, S. Hashiguchi, A. Fujii, T. Ikariya and R. Noyori, *Angew. Chem., Int. Ed. Engl.*, 1997, **36**, 285; (b) R. Noyori, M. Yamakawa and S. Hashiguchi, *J. Org. Chem.*, 2001, **66**, 7931; (c) T. Ikariya and A. J. Blacker, *Acc. Chem. Res.*, 2007, **40**, 1300; (d) T. Ikariya, *Bull. Chem. Soc. Jpn.*, 2011, **84**, 1; (e) P. A. Dub and J. C. Gordon, *Dalton Trans.*, 2016, **45**, 6756.
- S. Chakraborty, W. W. Brennessel and W. D. Jones, *J. Am. Chem. Soc.*, 2014, **136**, 8564.
- S. Chakraborty, P. O. Lagaditis, M. Förster, E. A. Bielinski, N. Hazari, M. C. Holthausen, W. D. Jones and S. Schneider, *ACS Catal.*, 2014, **4**, 3994.
- P. O. Lagaditis, P. E. Sues, J. F. Sonnenberg, K. Y. Wan, A. J. Lough and R. H. Morris, *J. Am. Chem. Soc.*, 2014, **136**, 1367.
- S. A. M. Smith, P. O. Lagaditis, A. Lüpke, A. J. Lough and R. H. Morris, *Chem. – Eur. J.*, 2017, **23**, 7212.
- A. Zirakzadeh, K. Kirchner, A. Roller, B. Stöger, M. Widhalm and R. H. Morris, *Organometallics*, 2016, **35**, 3781.
- H. U. Blaser, *Chem. Rev.*, 1992, **92**, 935.
- M. D. Fryzuk and B. Bosnich, *J. Am. Chem. Soc.*, 1977, **99**, 6262.
- R. S. Cahn, C. Ingold and V. Prelog, *Angew. Chem.*, 1966, **78**, 413.
- (a) H. Brunner, A. Winter and J. Breu, *J. Organomet. Chem.*, 1998, **553**, 285. For definitions, see: (b) D. Cremer, *Isr. J. Chem.*, 1980, **20**, 12.
- (a) W. S. Knowles, M. J. Sabacky, B. D. Vineyard and D. J. Weinkauff, *J. Am. Chem. Soc.*, 1975, **97**, 2567; (b) B. D. Vineyard, W. S. Knowles, M. J. Sabacky, G. L. Bachman and D. J. Weinkauff, *J. Am. Chem. Soc.*, 1977, **99**, 5946.
- For early studies, see: C. L. Landis and J. Halpern, *J. Am. Chem. Soc.*, 1987, **109**, 1746, and references therein.
- (a) I. D. Gridnev and T. Imamoto, *Acc. Chem. Res.*, 2004, **37**, 633. For a discussion of attraction vs. repulsion, see: (b) I. D. Gridnev, *ChemCatChem*, 2016, **8**, 3463.
- J. S. Giovannetti, C. M. Kelly and C. R. Landis, *J. Am. Chem. Soc.*, 1993, **115**, 4040.
- W. S. Knowles, *Acc. Chem. Res.*, 1983, **16**, 106.
- H. Tsuruta, T. Imamoto, K. Yamaguchi and I. D. Gridnev, *Tetrahedron Lett.*, 2005, **46**, 2879.
- (a) B. Zupancic, B. Mohar and M. Stephan, *Adv. Synth. Catal.*, 2008, **350**, 2024; (b) M. Stephan, D. Šterk and B. Mohar, *Adv. Synth. Catal.*, 2009, **351**, 2779; (c) B. Zupančič, B. Mohar and M. Stephan, *Org. Lett.*, 2010, **12**, 1296.
- F. Maienza, F. Spindler, M. Thommen, B. Pugin, C. Malan and A. Mezzetti, *J. Org. Chem.*, 2002, **67**, 5239.
- Asymmetric hydrogenation of functionalised olefins: (a) T. Imamoto, J. Watanabe, Y. Wada, H. Masuda, H. Yamada, H. Tsuruta, S. Matsukawa and K. Yamaguchi, *J. Am. Chem. Soc.*, 1998, **120**, 1635; (b) A. Ohashi and T. Imamoto, *Org. Lett.*, 2001, **3**, 373; (c) A. Ohashi, S. I. Kikuchi, M. Yasutake and T. Imamoto, *Eur. J. Org. Chem.*, 2002, 2535. Arylation of enones: (d) T. Imamoto, Y. Saitoh, A. Koide, T. Ogura and K. Yoshida, *Angew. Chem., Int. Ed.*, 2007, **46**, 8636. Iridium-catalysed imine hydrogenation: (e) T. Imamoto, N. Iwade and K. Yoshida, *Org. Lett.*, 2006, **8**, 2289. Ruthenium-catalysed asymmetric hydrogenation of  $\beta$ -ketoesters: (f) T. Yamano, N. Taya, M. Kawada, T. Huang and T. Imamoto, *Tetrahedron Lett.*, 1999, **40**, 2577. Pd-catalysed allylic alkylation: (g) N. Oohara, K. Katagiri and T. Imamoto, *Tetrahedron: Asymmetry*, 2003, **14**, 2171.
- I. D. Gridnev, Y. Yamanoi, N. Higashi, H. Tsuruta, M. Yasutake and T. Imamoto, *Adv. Synth. Catal.*, 2001, **343**, 118.
- Y. Yamanoi and T. Imamoto, *J. Org. Chem.*, 1999, **64**, 2988.
- I. D. Gridnev, M. Yasutake, N. Higashi and T. Imamoto, *J. Am. Chem. Soc.*, 2001, **123**, 5268.
- (a) G. Hoge, H. P. Wu, W. S. Kissel, D. A. Pflum, D. J. Greene and J. Bao, *J. Am. Chem. Soc.*, 2004, **126**, 5966; (b) H. P. Wu and G. Hoge, *Org. Lett.*, 2004, **6**, 3645; (c) I. D. Gridnev, T. Imamoto, G. Hoge, M. Kouchi and H. Takahashi, *J. Am. Chem. Soc.*, 2008, **130**, 2560.
- (a) E. Cristobal-Lecina, P. Etayo, S. Doran, M. Revés, P. Martin-Gago, A. Grabulosa, A. R. Costantino, A. Vidal-Ferran, A. Riera and X. Verdager, *Adv. Synth. Catal.*, 2014, **356**, 795; (b) E. Cristobal-Lecina, A. R. Costantino, A. Grabulosa, A. Riera and X. Verdager, *Organometallics*, 2015, **34**, 4989.
- K. Mislow and J. Siegel, *J. Am. Chem. Soc.*, 1984, **106**, 3319.
- (a) M. J. Burk, J. E. Feaster, W. A. Nugent and R. L. Harlow, *J. Am. Chem. Soc.*, 1993, **115**, 10125. See also: (b) S. Rast, M. Stephan and B. Mohar, *Eur. J. Org. Chem.*, 2015, 2214.
- (a) T. Miura and T. Imamoto, *Tetrahedron Lett.*, 1999, **40**, 4833; (b) K. Tamura, M. Sugiyama, K. Yoshida, A. Yanagisawa and T. Imamoto, *Org. Lett.*, 2010, **12**, 4400.
- T. Imamoto, K. Sugita and K. Yoshida, *J. Am. Chem. Soc.*, 2005, **127**, 11934.
- Functionalised alkenes: (a) T. Imamoto, K. Tamura, Z. Zhang, Y. Horiuchi, M. Sugiyama, K. Yoshida, A. Yanagisawa and I. D. Gridnev,





- J. Am. Chem. Soc.*, 2012, **134**, 1754. Functionalised  $\alpha$ -dehydroamino ketones: (b) Q. Hu, J. Chen, Z. Zhang, Y. Liu and W. Zhang, *Org. Lett.*, 2016, **18**, 1290. Allylic hydrazones: (c) Q. P. Hu, Y. H. Hu, Y. Liu, Z. F. Zhang, Y. G. Liu and W. B. Zhang, *Chem. – Eur. J.*, 2017, **23**, 1040.
- 52 Y. Shibata and K. Tanaka, *J. Am. Chem. Soc.*, 2009, **131**, 12552.
- 53 I. H. Chen, L. Yin, W. Itano, M. Kanai and M. Shibasaki, *J. Am. Chem. Soc.*, 2009, **131**, 11664.
- 54 (a) K. Kubota, E. Yamamoto and H. Ito, *Adv. Synth. Catal.*, 2013, **355**, 3527; (b) E. Yamamoto, Y. Takenouchi, T. Ozaki, T. Miya and H. Ito, *J. Am. Chem. Soc.*, 2014, **136**, 16515; (c) K. Kubota, Y. Watanabe and H. Ito, *Adv. Synth. Catal.*, 2016, **358**, 2379.
- 55 (a) K. Yao, D. Liu, Q. Yuan, T. Imamoto, Y. Liu and W. Zhang, *Org. Lett.*, 2016, **18**, 6296; (b) T. Imamoto, M. Nishimura, A. Koide and K. Yoshida, *J. Org. Chem.*, 2007, **72**, 7413.
- 56 M. Jin, L. Adak and M. Nakamura, *J. Am. Chem. Soc.*, 2015, **137**, 7128.
- 57 S. I. Featherman and L. D. Quin, *J. Am. Chem. Soc.*, 1975, **97**, 4349.
- 58 C. R. Johnson and T. Imamoto, *J. Org. Chem.*, 1987, **52**, 2170.
- 59 T. Imamoto, Y. Horiuchi, E. Hamanishi, S. Takeshita, K. Tamura, M. Sugiyama and K. Yoshida, *Tetrahedron*, 2015, **71**, 6471.
- 60 J. Bakos, I. Toth, B. Heil, G. Szalontai, L. Parkanyi and V. Fülöp, *J. Organomet. Chem.*, 1989, **370**, 263.
- 61 R. M. Stoop, F. Spindler and A. Mezzetti, *Organometallics*, 1998, **17**, 668.
- 62 J. Holz, K. Rumpel, A. Spannenberg, R. Paciello, H. J. Jiao and A. Börner, *ACS Catal.*, 2017, **7**, 6162.
- 63 (a) U. Nettekoven, P. C. J. Kamer, P. W. N. M. van Leeuwen, M. Widhalm, A. L. Spek and M. Lutz, *J. Org. Chem.*, 1999, **64**, 3996; (b) F. Maienza, M. Wörle, P. Steffanut, A. Mezzetti and F. Spindler, *Organometallics*, 1999, **18**, 1041.
- 64 E. Salomó, A. Gallen, G. Sciortino, G. Ujaque, A. Grabulosa, A. Lledós, A. Riera and X. Verdager, *J. Am. Chem. Soc.*, 2018, **140**, 16967.
- 65 (a) S. Jugé, M. Stephan, J. A. Laffitte and J. P. Genêt, *Tetrahedron Lett.*, 1990, **31**, 6357; (b) S. Jugé, M. Stephan, R. Merdès, J. P. Genêt and S. Hault-Desportes, *J. Chem. Soc., Chem. Commun.*, 1993, 531; (c) S. Jugé, *Phosphorus, Sulfur Silicon Relat. Elem.*, 2008, **183**, 233.
- 66 A. R. Muci, K. R. Campos and D. A. Evans, *J. Am. Chem. Soc.*, 1995, **117**, 9075.
- 67 K. Nagata, S. Matsukawa and T. Imamoto, *J. Org. Chem.*, 2000, **65**, 4185.
- 68 Q. Xu, C. Q. Zhao and L. B. Han, *J. Am. Chem. Soc.*, 2008, **130**, 12648.
- 69 M. Stephan, B. Sterk, B. Modéc and B. Mohar, *J. Org. Chem.*, 2007, **72**, 8010.
- 70 E. B. Kaloun, R. Merdès, J. P. Genêt, J. Uziel and S. Jugé, *J. Organomet. Chem.*, 1997, **529**, 455.
- 71 G. C. Lloyd-Jones and N. P. Taylor, *Chem. – Eur. J.*, 2015, **21**, 5423.
- 72 L. McKinstry and T. Livinghouse, *Tetrahedron Lett.*, 1994, **35**, 9319.
- 73 T. Imamoto, *Chem. Rec.*, 2016, **16**, 2659.
- 74 K. M. M. Huihui, R. Shrestha and D. J. Weix, *Org. Lett.*, 2017, **19**, 340.
- 75 L. Horner, H. Winkler, A. Rapp, A. Mentrup, H. Hoffmann and P. Beck, *Tetrahedron Lett.*, 1961, **2**, 161.
- 76 (a) O. Korpium and K. Mislow, *J. Am. Chem. Soc.*, 1967, **89**, 4784; (b) O. Korpium, R. A. Lewis, J. Chickos and K. Mislow, *J. Am. Chem. Soc.*, 1968, **90**, 4842.
- 77 K. M. Pietrusiewicz and M. Zablocka, *Chem. Rev.*, 1994, **94**, 1375.
- 78 T. L. Emmick and R. L. Letsinger, *J. Am. Chem. Soc.*, 1968, **90**, 3459.
- 79 H. Y. Su and M. S. Taylor, *J. Org. Chem.*, 2017, **82**, 3173.
- 80 R. Bigler and A. Mezzetti, *Org. Process Res. Dev.*, 2016, **20**, 253.
- 81 D. Hérault, D. C. Nguyen, D. Nuel and G. Buono, *Chem. Soc. Rev.*, 2015, **44**, 2508.
- 82 (a) G. X. Zhu, M. Terry and X. M. Zhang, *Tetrahedron Lett.*, 1996, **37**, 4475; (b) G. X. Zhu, M. Terry and X. M. Zhang, *J. Organomet. Chem.*, 1997, **547**, 97.
- 83 B. Wolfe and T. Livinghouse, *J. Am. Chem. Soc.*, 1998, **120**, 5116.
- 84 I. Arenas, O. Boutureira, M. I. Matheu, Y. Diaz and S. Castillon, *Eur. J. Org. Chem.*, 2015, 3666.
- 85 (a) T. Miura, H. Yamada, S. I. Kikuchi and T. Imamoto, *J. Org. Chem.*, 2000, **65**, 1877; (b) Y. Zhu, Z. H. Yang, B. Q. Ding, D. L. Liu, Y. G. Liu, M. Sugiyama, T. Imamoto and W. B. Zhang, *Tetrahedron*, 2015, **71**, 6832; (c) Z. H. Yang, X. Wei, D. L. Liu, Y. G. Liu, M. Sugiyama, T. Imamoto and W. B. Zhang, *J. Organomet. Chem.*, 2015, **791**, 41; (d) Z. H. Yang, D. L. Liu, G. Liu, M. Sugiyama, T. Imamoto and W. B. Zhang, *Organometallics*, 2015, **34**, 1228; (e) Z. H. Yang, C. Xia, D. L. Liu, Y. G. Liu, M. Sugiyama, T. Imamoto and W. B. Zhang, *Org. Biomol. Chem.*, 2015, **13**, 2694.
- 86 (a) B. S. Williams, P. Dani, M. Lutz, A. L. Spek and G. van Koten, *Helv. Chim. Acta*, 2001, **84**, 3519. See also: (b) D. Morales-Morales, R. E. Cramer and C. M. Jensen, *J. Organomet. Chem.*, 2002, **654**, 44; (c) S. Medici, M. Gagliardo, S. B. Williams, P. A. Chase, S. Gladiali, M. Lutz, A. L. Spek, G. P. M. van Klink and G. van Koten, *Helv. Chim. Acta*, 2005, **88**, 694.
- 87 B. Q. Ding, Z. F. Zhang, Y. Xu, Y. G. Liu, M. Sugiyama, T. Imamoto and W. B. Zhang, *Org. Lett.*, 2013, **15**, 5476.
- 88 R. Huber, A. Passera and A. Mezzetti, *Organometallics*, 2018, **37**, 396.
- 89 R. Huber, *Iron meets stereogenic phosphorus: Fe(II) catalysts with chiral NPPN and PNP ligands*, PhD thesis, ETH Zürich, 2018.
- 90 R. Huber, A. Passera and A. Mezzetti, *Adv. Synth. Catal.*, 2018, **360**, 2990.
- 91 T. Imamoto, M. Matsuo, T. Nonomura, K. Kishikawa and M. Yanagawa, *Heteroat. Chem.*, 1993, **4**, 475.
- 92 S. Lemouzy, D. H. Nguyen, V. Camy, M. Jean, D. Gatineau, L. Giordano, J. V. Naubron, N. Vanthuyne, D. Hérault and G. Buono, *Chem. – Eur. J.*, 2015, **21**, 15607.
- 93 W. M. Wang, L. J. Liu, C. Q. Zhao and L. B. Han, *Eur. J. Org. Chem.*, 2015, 2342.
- 94 S. Sowa, M. Stankevič, A. Szmigielska, H. Małuszyńska, A. E. Koziol and K. M. Pietrusiewicz, *J. Org. Chem.*, 2015, **80**, 1672.
- 95 (a) V. S. Chan, I. C. Stewart, R. G. Bergman and F. D. Toste, *J. Am. Chem. Soc.*, 2006, **128**, 2786; (b) V. S. Chan, M. Chiu, R. G. Bergman and F. D. Toste, *J. Am. Chem. Soc.*, 2009, **131**, 6021.
- 96 (a) X. Z. Yang, *Inorg. Chem.*, 2011, **50**, 12836; (b) G. R. Morello and K. H. Hopmann, *ACS Catal.*, 2017, **7**, 5847.
- 97 R. Langer, M. A. Iron, L. Konstantinovskii, Y. Diskin-Posner, G. Leituss, Y. Ben-David and D. Milstein, *Chem. – Eur. J.*, 2012, **18**, 7196.
- 98 J. I. Seeman, *Chem. Rev.*, 1983, **83**, 83.

